Biomedical Optics EXPRESS

Imaging axonal transport in the rat visual pathway

Carla J. Abbott,[1] Tiffany E. Choe,[1] Theresa A. Lusardi,[2] Claude F. Burgoyne,[1] Lin Wang,[1] and Brad Fortune[1,*]

[1]*Discoveries in Sight Research Laboratories, Devers Eye Institute, and Legacy Research Institute, Legacy Health, Portland, OR 97232, USA*

[2]*R.S. Dow Neurobiology Laboratories, Legacy Research Institute, Legacy Health, Portland, OR 97232, USA*

**bfortune@deverseye.org*

Abstract: A technique was developed for assaying axonal transport in retinal ganglion cells using 2 µl injections of 1% cholera toxin b-subunit conjugated to AlexaFluor488 (CTB). *In vivo* retinal and post-mortem brain imaging by confocal scanning laser ophthalmoscopy and post-mortem microscopy were performed. The transport of CTB was sensitive to colchicine, which disrupts axonal microtubules. The bulk rates of transport were determined to be approximately 80–90 mm/day (anterograde) and 160 mm/day (retrograde). Results demonstrate that axonal transport of CTB can be monitored *in vivo* in the rodent anterior visual pathway, is dependent on intact microtubules, and occurs by active transport mechanisms.

OCIS codes: (170.2655) Functional monitoring and imaging; (170.3880) Medical and biological imaging.

References and links

1. A. Brown, "Axonal transport of membranous and nonmembranous cargoes: a unified perspective," J. Cell Biol. **160**(6), 817–821 (2003).
2. R. D. Vale and R. A. Milligan, "The way things move: looking under the hood of molecular motor proteins," Science **288**(5463), 88–95 (2000).
3. A. J. Reynolds, S. E. Bartlett, and I. A. Hendry, "Molecular mechanisms regulating the retrograde axonal transport of neurotrophins," Brain Res. Brain Res. Rev. **33**(2-3), 169–178 (2000).
4. P. J. Hollenbeck and W. M. Saxton, "The axonal transport of mitochondria," J. Cell Sci. **118**(23), 5411–5419 (2005).
5. C. Balaratnasingam, W. H. Morgan, L. Bass, G. Matich, S. J. Cringle, and D. Y. Yu, "Axonal transport and cytoskeletal changes in the laminar regions after elevated intraocular pressure," Invest. Ophthalmol. Vis. Sci. **48**(8), 3632–3644 (2007).
6. C. Balaratnasingam, W. H. Morgan, L. Bass, L. Ye, C. McKnight, S. J. Cringle, and D. Y. Yu, "Elevated pressure induced astrocyte damage in the optic nerve," Brain Res. **1244**, 142–154 (2008).
7. J. O. Johansson, "Retrograde axoplasmic transport in rat optic nerve *in vivo*. What causes blockage at increased intraocular pressure?" Exp. Eye Res. **43**(4), 653–660 (1986).
8. J. O. Johansson, "Inhibition and recovery of retrograde axoplasmic transport in rat optic nerve during and after elevated IOP *in vivo*," Exp. Eye Res. **46**(2), 223–227 (1988).
9. H. A. Quigley, S. J. McKinnon, D. J. Zack, M. E. Pease, L. A. Kerrigan-Baumrind, D. F. Kerrigan, and R. S. Mitchell, "Retrograde axonal transport of BDNF in retinal ganglion cells is blocked by acute IOP elevation in rats," Invest. Ophthalmol. Vis. Sci. **41**(11), 3460–3466 (2000).
10. M. E. Pease, S. J. McKinnon, H. A. Quigley, L. A. Kerrigan-Baumrind, and D. J. Zack, "Obstructed axonal transport of BDNF and its receptor TrkB in experimental glaucoma," Invest. Ophthalmol. Vis. Sci. **41**(3), 764–774 (2000).
11. D. R. Anderson and A. Hendrickson, "Effect of intraocular pressure on rapid axoplasmic transport in monkey optic nerve," Invest. Ophthalmol. **13**(10), 771–783 (1974).
12. H. Quigley and D. R. Anderson, "The dynamics and location of axonal transport blockade by acute intraocular pressure elevation in primate optic nerve," Invest. Ophthalmol. **15**(8), 606–616 (1976).
13. H. A. Quigley, J. Guy, and D. R. Anderson, "Blockade of rapid axonal transport. Effect of intraocular pressure elevation in primate optic nerve," Arch. Ophthalmol. **97**(3), 525–531 (1979).
14. R. L. Radius and D. R. Anderson, "Breakdown of the normal optic nerve head blood-brain barrier following acute elevation of intraocular pressure in experimental animals," Invest. Ophthalmol. Vis. Sci. **19**(3), 244–255 (1980).

#178418 - $15.00 USD Received 19 Nov 2012; revised 10 Jan 2013; accepted 28 Jan 2013; published 30 Jan 2013

15. H. A. Quigley and D. R. Anderson, "Distribution of axonal transport blockade by acute intraocular pressure elevation in the primate optic nerve head," Invest. Ophthalmol. Vis. Sci. **16**(7), 640–644 (1977).
16. R. L. Radius, E. L. Schwartz, and D. R. Anderson, "Failure of unilateral carotid artery ligation to affect pressure-induced interruption of rapid axonal transport in primate optic nerves," Invest. Ophthalmol. Vis. Sci. **19**(2), 153–157 (1980).
17. D. S. Minckler, A. H. Bunt, and G. W. Johanson, "Orthograde and retrograde axoplasmic transport during acute ocular hypertension in the monkey," Invest. Ophthalmol. Vis. Sci. **16**(5), 426–441 (1977).
18. D. S. Minckler, A. H. Bunt, and I. B. Klock, "Radioautographic and cytochemical ultrastructural studies of axoplasmic transport in the monkey optic nerve head," Invest. Ophthalmol. Vis. Sci. **17**(1), 33–50 (1978).
19. D. Gaasterland, T. Tanishima, and T. Kuwabara, "Axoplasmic flow during chronic experimental glaucoma. 1. Light and electron microscopic studies of the monkey optic nervehead during development of glaucomatous cupping," Invest. Ophthalmol. Vis. Sci. **17**(9), 838–846 (1978).
20. P. W. Lampert, M. H. Vogel, and L. E. Zimmerman, "Pathology of the optic nerve in experimental acute glaucoma. Electron microscopic studies," Invest. Ophthalmol. **7**(2), 199–213 (1968).
21. R. L. Radius and D. R. Anderson, "Reversibility of optic nerve damage in primate eyes subjected to intraocular pressure above systolic blood pressure," Br. J. Ophthalmol. **65**(10), 661–672 (1981).
22. R. L. Radius and D. R. Anderson, "Rapid axonal transport in primate optic nerve. Distribution of pressure-induced interruption," Arch. Ophthalmol. **99**(4), 650–654 (1981).
23. H. A. Quigley and E. M. Addicks, "Chronic experimental glaucoma in primates. II. Effect of extended intraocular pressure elevation on optic nerve head and axonal transport," Invest. Ophthalmol. Vis. Sci. **19**(2), 137–152 (1980).
24. L. Dandona, A. Hendrickson, and H. A. Quigley, "Selective effects of experimental glaucoma on axonal transport by retinal ganglion cells to the dorsal lateral geniculate nucleus," Invest. Ophthalmol. Vis. Sci. **32**(5), 1593–1599 (1991).
25. K. R. G. Martin, H. A. Quigley, D. Valenta, J. Kielczewski, and M. E. Pease, "Optic nerve dynein motor protein distribution changes with intraocular pressure elevation in a rat model of glaucoma," Exp. Eye Res. **83**(2), 255–262 (2006).
26. G. Chidlow, A. Ebneter, J. P. M. Wood, and R. J. Casson, "The optic nerve head is the site of axonal transport disruption, axonal cytoskeleton damage and putative axonal regeneration failure in a rat model of glaucoma," Acta Neuropathol. **121**(6), 737–751 (2011).
27. S. D. Crish, R. M. Sappington, D. M. Inman, P. J. Horner, and D. J. Calkins, "Distal axonopathy with structural persistence in glaucomatous neurodegeneration," Proc. Natl. Acad. Sci. U.S.A. **107**(11), 5196–5201 (2010).
28. M. Salinas-Navarro, L. Alarcón-Martínez, F. J. Valiente-Soriano, M. Jiménez-López, S. Mayor-Torroglosa, M. Avilés-Trigueros, M. P. Villegas-Pérez, and M. Vidal-Sanz, "Ocular hypertension impairs optic nerve axonal transport leading to progressive retinal ganglion cell degeneration," Exp. Eye Res. **90**(1), 168–183 (2010).
29. Y. Munemasa, Y. Kitaoka, J. Kuribayashi, and S. Ueno, "Modulation of mitochondria in the axon and soma of retinal ganglion cells in a rat glaucoma model," J. Neurochem. **115**(6), 1508–1519 (2010).
30. I. Soto, E. Oglesby, B. P. Buckingham, J. L. Son, E. D. O. Roberson, M. R. Steele, D. M. Inman, M. L. Vetter, P. J. Horner, and N. Marsh-Armstrong, "Retinal ganglion cells downregulate gene expression and lose their axons within the optic nerve head in a mouse glaucoma model," J. Neurosci. **28**(2), 548–561 (2008).
31. T. Misgeld, M. Kerschensteiner, F. M. Bareyre, R. W. Burgess, and J. W. Lichtman, "Imaging axonal transport of mitochondria *in vivo*," Nat. Methods **4**(7), 559–561 (2007).
32. Y. Takihara, M. Inatani, H. Hayashi, N. Adachi, K. Iwao, T. Inoue, M. Iwao, and H. Tanihara, "Dynamic imaging of axonal transport in living retinal ganglion cells *in vitro*," Invest. Ophthalmol. Vis. Sci. **52**(6), 3039–3045 (2011).
33. X. C. Wan, J. Q. Trojanowski, and J. O. Gonatas, "Cholera toxin and wheat germ agglutinin conjugates as neuroanatomical probes: their uptake and clearance, transganglionic and retrograde transport and sensitivity," Brain Res. **243**(2), 215–224 (1982).
34. J. Q. Trojanowski, J. O. Gonatas, and N. K. Gonatas, "Horseradish peroxidase (HRP) conjugates of cholera toxin and lectins are more sensitive retrogradely transported markers than free HRP," Brain Res. **231**(1), 33–50 (1982).
35. P. H. Luppi, P. Fort, and M. Jouvet, "Iontophoretic application of unconjugated cholera toxin B subunit (CTb) combined with immunohistochemistry of neurochemical substances: a method for transmitter identification of retrogradely labeled neurons," Brain Res. **534**(1-2), 209–224 (1990).
36. C. C. Wu, R. M. Russell, and H. J. Karten, "The transport rate of cholera toxin B subunit in the retinofugal pathways of the chick," Neuroscience **92**(2), 665–676 (1999).
37. C. C. Wu, R. M. Russell, R. T. Nguyen, and H. J. Karten, "Tracing developing pathways in the brain: a comparison of carbocyanine dyes and cholera toxin b subunit," Neuroscience **117**(4), 831–845 (2003).
38. S. Reuss and K. Decker, "Anterograde tracing of retinohypothalamic afferents with Fluoro-Gold," Brain Res. **745**(1-2), 197–204 (1997).
39. M. D. Fleming, R. M. Benca, and M. Behan, "Retinal projections to the subcortical visual system in congenic albino and pigmented rats," Neuroscience **143**(3), 895–904 (2006).
40. N. Rivera and N. Lugo, "Four retinal ganglion cell types that project to the superior colliculus in the thirteen-lined ground squirrel (*Spermophilus tridecemlineatus*)," J. Comp. Neurol. **396**(1), 105–120 (1998).
41. M. E. Schwab and H. Thoenen, "Retrograde axonal and transsynaptic transport of macromolecules: physiological and pathophysiological importance," Agents Actions **7**(3), 361–368 (1977).

#178418 - $15.00 USD Received 19 Nov 2012; revised 10 Jan 2013; accepted 28 Jan 2013; published 30 Jan 2013

42. J. D. Mikkelsen, "Visualization of efferent retinal projections by immunohistochemical identification of cholera toxin subunit B," Brain Res. Bull. **28**(4), 619–623 (1992).
43. A. Angelucci, F. Clascá, and M. Sur, "Anterograde axonal tracing with the subunit B of cholera toxin: a highly sensitive immunohistochemical protocol for revealing fine axonal morphology in adult and neonatal brains," J. Neurosci. Methods **65**(1), 101–112 (1996).
44. N. K. Gonatas, A. Stieber, J. Gonatas, T. Mommoi, and P. H. Fishman, "Endocytosis of exogenous GM1 ganglioside and cholera toxin by neuroblastoma cells," Mol. Cell. Biol. **3**(1), 91–101 (1983).
45. K. C. Joseph, S. U. Kim, A. Stieber, and N. K. Gonatas, "Endocytosis of cholera toxin into neuronal GERL," Proc. Natl. Acad. Sci. U.S.A. **75**(6), 2815–2819 (1978).
46. M. Hirakawa, J. T. McCabe, and M. Kawata, "Time-related changes in the labeling pattern of motor and sensory neurons innervating the gastrocnemius muscle, as revealed by the retrograde transport of the cholera toxin B subunit," Cell Tissue Res. **267**(3), 419–427 (1992).
47. S. Ochs, "Fast transport of materials in mammalian nerve fibers," Science **176**(4032), 252–260 (1972).
48. S. Inoue, "The effect of colchicine on the microscopic and submicroscopic structure of the mitotic spindle," Exp. Cell Res. Suppl. **2**, 305–318 (1952).
49. O. J. Eigsti, "A cytological study of colchicine effects in the induction of polyploidy in plants," Proc. Natl. Acad. Sci. U.S.A. **24**(2), 56–63 (1938).
50. O. J. Eigsti and P. D. Dustin, Jr., *Colchicine— in Agriculture, Medicine, Biology and Chemistry* (Iowa State College Press, Ames, IA, 1955)
51. A. Dahlström, "Effect of colchicine on transport of amine storage granules in sympathetic nerves of rat," Eur. J. Pharmacol. **5**(1), 111–113 (1968).
52. G. W. Kreutzberg, "Neuronal dynamics and axonal flow. IV. Blockage of intra-axonal enzyme transport by colchicine," Proc. Natl. Acad. Sci. U.S.A. **62**(3), 722–728 (1969).
53. J. O. Karlsson and J. Sjöstrand, "The effect of colchicine on the axonal transport of protein in the optic nerve and tract of the rabbit," Brain Res. **13**(3), 617–619 (1969).
54. K. A. James, J. J. Bray, I. G. Morgan, and L. Austin, "The effect of colchicine on the transport of axonal protein in the chicken," Biochem. J. **117**(4), 767–771 (1970).
55. B. Fortune, L. Wang, G. Cull, and G. A. Cioffi, "Intravitreal colchicine causes decreased RNFL birefringence without altering RNFL thickness," Invest. Ophthalmol. Vis. Sci. **49**(1), 255–261 (2008).
56. J. O. Karlsson, H. A. Hansson, and J. Sjöstrand, "Effect of colchicine on axonal transport and morphology of retinal ganglion cells," Z. Zellforsch. Mikrosk. Anat. **115**(2), 265–283 (1971).
57. I. G. Morgan, "Intraocular colchicine selectively destroys immature ganglion cells in chicken retina," Neurosci. Lett. **24**(3), 255–260 (1981).
58. C. Davidson, W. R. Green, and V. G. Wong, "Retinal atrophy induced by intravitreous colchicine," Invest. Ophthalmol. Vis. Sci. **24**(3), 301–311 (1983).
59. M. G. Honig and R. I. Hume, "Fluorescent carbocyanine dyes allow living neurons of identified origin to be studied in long-term cultures," J. Cell Biol. **103**(1), 171–187 (1986).
60. R. D. Lund and S. D. Hauschka, "Transplanted neural tissue develops connections with host rat brain," Science **193**(4253), 582–584 (1976).
61. P. W. Land and R. D. Lund, "Development of the rat's uncrossed retinotectal pathway and its relation to plasticity studies," Science **205**(4407), 698–700 (1979).
62. F. Mazzoni, E. Novelli, and E. Strettoi, "Retinal ganglion cells survive and maintain normal dendritic morphology in a mouse model of inherited photoreceptor degeneration," J. Neurosci. **28**(52), 14282–14292 (2008).
63. U. C. Dräger and D. H. Hubel, "Topography of visual and somatosensory projections to mouse superior colliculus," J. Neurophysiol. **39**(1), 91–101 (1976).
64. M. Vidal-Sanz, M. P. Villegas-Pérez, G. M. Bray, and A. J. Aguayo, "Persistent retrograde labeling of adult rat retinal ganglion cells with the carbocyanine dye diI," Exp. Neurol. **102**(1), 92–101 (1988).
65. S. Thanos, J. Kacza, J. Seeger, and J. Mey, "Old dyes for new scopes: the phagocytosis-dependent long-term fluorescence labelling of microglial cells *in vivo*," Trends Neurosci. **17**(5), 177–182 (1994).
66. L. C. Katz, A. Burkhalter, and W. J. Dreyer, "Fluorescent latex microspheres as a retrograde neuronal marker for *in vivo* and *in vitro* studies of visual cortex," Nature **310**(5977), 498–500 (1984).
67. J. J. Quattrochi, A. N. Mamelak, R. D. Madison, J. D. Macklis, and J. A. Hobson, "Mapping neuronal inputs to REM sleep induction sites with carbachol-fluorescent microspheres," Science **245**(4921), 984–986 (1989).
68. G. C. Walter, R. J. Phillips, E. A. Baronowsky, and T. L. Powley, "Versatile, high-resolution anterograde labeling of vagal efferent projections with dextran amines," J. Neurosci. Methods **178**(1), 1–9 (2009).
69. J. Lu, P. Shiromani, and C. B. Saper, "Retinal input to the sleep-active ventrolateral preoptic nucleus in the rat," Neuroscience **93**(1), 209–214 (1999).
70. P. H. Luppi, K. Sakai, D. Salvert, P. Fort, and M. Jouvet, "Peptidergic hypothalamic afferents to the cat nucleus raphe pallidus as revealed by a double immunostaining technique using unconjugated cholera toxin as a retrograde tracer," Brain Res. **402**(2), 339–345 (1987).
71. G. R. Howell, I. Soto, X. Zhu, M. Ryan, D. G. Macalinao, G. L. Sousa, L. B. Caddle, K. H. MacNicoll, J. M. Barbay, V. Porciatti, M. G. Anderson, R. S. Smith, A. F. Clark, R. T. Libby, and S. W. John, "Radiation treatment inhibits monocyte entry into the optic nerve head and prevents neuronal damage in a mouse model of glaucoma," J. Clin. Invest. **122**(4), 1246–1261 (2012).

#178418 - $15.00 USD Received 19 Nov 2012; revised 10 Jan 2013; accepted 28 Jan 2013; published 30 Jan 2013

72. S. Roy, P. Coffee, G. Smith, R. K. Liem, S. T. Brady, and M. M. Black, "Neurofilaments are transported rapidly but intermittently in axons: implications for slow axonal transport," J. Neurosci. **20**(18), 6849–6861 (2000).
73. L. Wang, C. L. Ho, D. Sun, R. K. H. Liem, and A. Brown, "Rapid movement of axonal neurofilaments interrupted by prolonged pauses," Nat. Cell Biol. **2**(3), 137–141 (2000).
74. M. M. Black and R. J. Lasek, "Slow components of axonal transport: two cytoskeletal networks," J. Cell Biol. **86**(2), 616–623 (1980).
75. J. E. Morgan, "Circulation and axonal transport in the optic nerve," Eye (Lond.) **18**(11), 1089–1095 (2004).
76. R. J. Lasek, J. A. Garner, and S. T. Brady, "Axonal transport of the cytoplasmic matrix," J. Cell Biol. **99**(1), 212s–221s (1984).
77. S. Roy, B. Zhang, V. M. Lee, and J. Q. Trojanowski, "Axonal transport defects: a common theme in neurodegenerative diseases," Acta Neuropathol. **109**(1), 5–13 (2005).
78. B. Grafstein and D. S. Forman, "Intracellular transport in neurons," Physiol. Rev. **60**(4), 1167–1283 (1980).
79. A. C. Breuer, M. P. Lynn, M. B. Atkinson, S. M. Chou, A. J. Wilbourn, K. E. Marks, J. E. Culver, and E. J. Fleegler, "Fast axonal transport in amyotrophic lateral sclerosis: an intra-axonal organelle traffic analysis," Neurology **37**(5), 738–748 (1987).
80. T. A. Viancour and N. A. Kreiter, "Vesicular fast axonal transport rates in young and old rat axons," Brain Res. **628**(1-2), 209–217 (1993).
81. T. Nakata, S. Terada, and N. Hirokawa, "Visualization of the dynamics of synaptic vesicle and plasma membrane proteins in living axons," J. Cell Biol. **140**(3), 659–674 (1998).
82. C. Kaether, P. Skehel, and C. G. Dotti, "Axonal membrane proteins are transported in distinct carriers: a two-color video microscopy study in cultured hippocampal neurons," Mol. Biol. Cell **11**(4), 1213–1224 (2000).
83. B. Fortune, G. A. Cull, and C. F. Burgoyne, "Relative course of retinal nerve fiber layer birefringence and thickness and retinal function changes after optic nerve transection," Invest. Ophthalmol. Vis. Sci. **49**(10), 4444–4452 (2008).
84. B. Fortune, C. F. Burgoyne, G. A. Cull, J. Reynaud, and L. Wang, "Structural and functional abnormalities of retinal ganglion cells measured *in vivo* at the onset of optic nerve head surface change in experimental glaucoma," Invest. Ophthalmol. Vis. Sci. **53**(7), 3939–3950 (2012).
85. X. R. Huang and R. W. Knighton, "Microtubules contribute to the birefringence of the retinal nerve fiber layer," Invest. Ophthalmol. Vis. Sci. **46**(12), 4588–4593 (2005).
86. X. R. Huang and R. W. Knighton, "Linear birefringence of the retinal nerve fiber layer measured *in vitro* with a multispectral imaging micropolarimeter," J. Biomed. Opt. **7**(2), 199–204 (2002).
87. Q. Zhou and R. W. Knighton, "Light scattering and form birefringence of parallel cylindrical arrays that represent cellular organelles of the retinal nerve fiber layer," Appl. Opt. **36**(10), 2273–2285 (1997).
88. B. A. Sabel, R. Engelmann, and M. F. Humphrey, "*In vivo* confocal neuroimaging (ICON) of CNS neurons," Nat. Med. **3**(2), 244–247 (1997).
89. R. Engelmann and B. A. Sabel, "*In vivo* imaging of mammalian central nervous system neurons with the *in vivo* confocal neuroimaging (ICON) method," Methods Enzymol. **307**, 563–570 (1999).
90. S. Thanos, L. Indorf, and R. Naskar, "*In vivo* FM: using conventional fluorescence microscopy to monitor retinal neuronal death *in vivo*," Trends Neurosci. **25**(9), 441–444 (2002).
91. M. F. Cordeiro, L. Guo, V. Luong, G. Harding, W. Wang, H. E. Jones, S. E. Moss, A. M. Sillito, and F. W. Fitzke, "Real-time imaging of single nerve cell apoptosis in retinal neurodegeneration," Proc. Natl. Acad. Sci. U.S.A. **101**(36), 13352–13356 (2004).
92. M. F. Cordeiro, L. Guo, K. M. Coxon, J. Duggan, S. Nizari, E. M. Normando, S. L. Sensi, A. M. Sillito, F. W. Fitzke, T. E. Salt, and S. E. Moss, "Imaging multiple phases of neurodegeneration: a novel approach to assessing cell death *in vivo*," Cell Death Dis **1**(1), e3 (2010).
93. L. Guo, T. E. Salt, A. Maass, V. Luong, S. E. Moss, F. W. Fitzke, and M. F. Cordeiro, "Assessment of neuroprotective effects of glutamate modulation on glaucoma-related retinal ganglion cell apoptosis *in vivo*," Invest. Ophthalmol. Vis. Sci. **47**(2), 626–633 (2006).
94. D. C. Gray, R. Wolfe, B. P. Gee, D. Scoles, Y. Geng, B. D. Masella, A. Dubra, S. Luque, D. R. Williams, and W. H. Merigan, "*In vivo* imaging of the fine structure of rhodamine-labeled macaque retinal ganglion cells," Invest. Ophthalmol. Vis. Sci. **49**(1), 467–473 (2008).
95. D. C. Gray, W. Merigan, J. I. Wolfing, B. P. Gee, J. Porter, A. Dubra, T. H. Twietmeyer, K. Ahamd, R. Tumbar, F. Reinholz, and D. R. Williams, "*In vivo* fluorescence imaging of primate retinal ganglion cells and retinal pigment epithelial cells," Opt. Express **14**(16), 7144–7158 (2006).
96. Y. Geng, K. P. Greenberg, R. Wolfe, D. C. Gray, J. J. Hunter, A. Dubra, J. G. Flannery, D. R. Williams, and J. Porter, "*In vivo* imaging of microscopic structures in the rat retina," Invest. Ophthalmol. Vis. Sci. **50**(12), 5872–5879 (2009).
97. C. K. S. Leung, J. D. Lindsey, J. G. Crowston, W. K. Ju, Q. Liu, D. U. Bartsch, and R. N. Weinreb, "*In vivo* imaging of murine retinal ganglion cells," J. Neurosci. Methods **168**(2), 475–478 (2008).
98. C. K. Leung, J. D. Lindsey, J. G. Crowston, C. Lijia, S. Chiang, and R. N. Weinreb, "Longitudinal profile of retinal ganglion cell damage after optic nerve crush with blue-light confocal scanning laser ophthalmoscopy," Invest. Ophthalmol. Vis. Sci. **49**(11), 4898–4902 (2008).
99. C. K. S. Leung and R. N. Weinreb, "Experimental detection of retinal ganglion cell damage *in vivo*," Exp. Eye Res. **88**(4), 831–836 (2009).

#178418 - $15.00 USD Received 19 Nov 2012; revised 10 Jan 2013; accepted 28 Jan 2013; published 30 Jan 2013

100. C. K. S. Leung, J. D. Lindsey, L. Chen, Q. Liu, and R. N. Weinreb, "Longitudinal profile of retinal ganglion cell damage assessed with blue-light confocal scanning laser ophthalmoscopy after ischaemic reperfusion injury," Br. J. Ophthalmol. **93**(7), 964–968 (2009).
101. C. K. Leung, R. N. Weinreb, Z. W. Li, S. Liu, J. D. Lindsey, N. Choi, L. Liu, C. Y. Cheung, C. Ye, K. Qiu, L. J. Chen, W. H. Yung, J. G. Crowston, M. Pu, K. F. So, C. P. Pang, and D. S. Lam, "Long-term *in vivo* imaging and measurement of dendritic shrinkage of retinal ganglion cells," Invest. Ophthalmol. Vis. Sci. **52**(3), 1539–1547 (2011).
102. T. Higashide, I. Kawaguchi, S. Ohkubo, H. Takeda, and K. Sugiyama, "*In vivo* imaging and counting of rat retinal ganglion cells using a scanning laser ophthalmoscope," Invest. Ophthalmol. Vis. Sci. **47**(7), 2943–2950 (2006).
103. M. K. Walsh and H. A. Quigley, "*In vivo* time-lapse fluorescence imaging of individual retinal ganglion cells in mice," J. Neurosci. Methods **169**(1), 214–221 (2008).
104. A. Kanamori, M. M. Catrinescu, M. Traistaru, R. Beaubien, and L. A. Levin, "*In vivo* imaging of retinal ganglion cell axons within the nerve fiber layer," Invest. Ophthalmol. Vis. Sci. **51**(4), 2011–2018 (2010).
105. H. Murata, M. Aihara, Y. N. Chen, T. Ota, J. Numaga, and M. Araie, "Imaging mouse retinal ganglion cells and their loss *in vivo* by a fundus camera in the normal and ischemia-reperfusion model," Invest. Ophthalmol. Vis. Sci. **49**(12), 5546–5552 (2008).
106. J. J. Gallagher, X. Zhang, G. J. Ziomek, R. E. Jacobs, and E. L. Bearer, "Deficits in axonal transport in hippocampal-based circuitry and the visual pathway in APP knock-out animals witnessed by manganese enhanced MRI," Neuroimage **60**(3), 1856–1866 (2012).
107. E. L. Bearer, T. L. Falzone, X. W. Zhang, O. Biris, A. Rasin, and R. E. Jacobs, "Role of neuronal activity and kinesin on tract tracing by manganese-enhanced MRI (MEMRI)," Neuroimage **37**(Suppl 1), S37–S46 (2007).
108. Y. Geng, A. Dubra, L. Yin, W. H. Merigan, R. Sharma, R. T. Libby, and D. R. Williams, "Adaptive optics retinal imaging in the living mouse eye," Biomed. Opt. Express **3**(4), 715–734 (2012).

1. Introduction

Axonal transport is critical to the growth, function and survival of neurons, as it enables metabolic messages (such as neurotrophic factors and neurotransmitters) to be passed between the cell soma and its axon terminals. Active axonal transport is performed primarily by molecular motor proteins (such as the family of kinesins for anterograde transport, and dynein for retrograde transport), which use cytoskeletal polymer tracks (microtubules or actin) to support the unidirectional movement of cargo molecules between proximal and distal regions of the axon [1–4]. Disruption of active axonal transport in retinal ganglion cells (RGCs) is thought to be a critical pathophysiological element of glaucomatous optic neuropathy and may even represent one of the earliest functional abnormalities affecting these cells [5–30]. Active axonal transport can be assayed using histopathological methods, but this requires sacrifice of the animal and typically time- and labor-intensive protocols involving tissue blocking, cutting and imaging of serial sections (see, e.g., [5,27].) Hence, development of more rapid axonal transport assays is desirable for use in experimental models of optic neuropathy, particularly if such assays can be accomplished *in vivo*. Indeed, development of an *in vivo* assay of axonal transport within RGCs could enable assessment of the pathophysiological role and sequence of transport obstruction in models of neurodegeneration such as glaucoma, and may allow evaluation of potential treatments to reverse transport deficits.

Recent reports have demonstrated development of novel techniques to examine active axonal transport *in vivo* and *in vitro*. For example, axonal transport of mitochondria in peripheral nerves of living transgenic mice and in acute explants has been imaged with time-lapse recordings [31] and live-cell imaging has revealed the transport dynamics of brain-derived neurotrophic factor (BDNF) in RGC axons and dendrites *in vitro* [32]. In addition, the availability of imaging tools such as confocal scanning laser ophthalmoscopy (CSLO) provide an opportunity to detect and quantify axonal transport tracers within the visual system *in vivo*.

One requirement for such an assay is that the tracer is carried primarily by active axonal transport rather than by simple diffusion through the neuronal/axonal cytosol or membrane. Work over the past two decades has raised the profile of cholera toxin subunit B (CTB) as an excellent candidate for use in axonal transport assays because of its high sensitivity, its capability to move in either anterograde or retrograde direction from the site of injection within a given neuronal tract, its restriction from labeling fibers of passage and its ability to

#178418 - $15.00 USD Received 19 Nov 2012; revised 10 Jan 2013; accepted 28 Jan 2013; published 30 Jan 2013

label the entire neuron, even fine processes and terminals in the mammalian nervous system including the visual pathway [33–43]. Its high sensitivity is thought to be due to the numerous binding sites (monosialoganglioside receptors, Gm1) on the surface of neurons [44,45].

Although CTB is often presumed to be transported by fast active mechanisms *in vivo*, there is actually considerable variability across the literature regarding the estimated rate of anterograde and retrograde transport of CTB [35,36,42,46]. Moreover, to our knowledge, there are no reports about the sensitivity of CTB to colchicine, which is a fundamental experiment for whether a tracer travels by active transport [47]. Colchicine is a compound that disrupts microtubules [48–50], therefore it can be used to assay the integrity of active axonal transport [32,47,51–54]. Microtubules within RGC axons are rapidly disrupted when colchicine is administered by intravitreal injection [55–58]. Hence, determining both the sensitivity of CTB axonal transport to intravitreal colchicine injection and the bulk rate of transport along the length of the axon are important experiments to confirm the transport mechanism of CTB.

Thus the overall aim of this study was to develop techniques imaging anterograde and retrograde active axonal transport in rodent RGC axons. Primarily, we used the well-known neuronal tract tracer CTB conjugated to a fluorescent marker appropriate for use with a commercially available CSLO, but also tested latex microspheres and a carbocyanine dye for comparison. Specifically, we tested the hypothesis that CTB is transported in both anterograde and retrograde directions by fast active mechanisms within RGC axons of the rat optic nerve. We performed two fundamental experiments to test this hypothesis, which have not previously been done: 1) we tested the dependence of CTB transport on intact microtubules by evaluating its sensitivity to colchicine treatment and 2) we tested the rate of transport (to be contrasted with slow active mechanisms and/or passive diffusion) [1,59].

2. Methods

2.1. Subjects

The subjects of this study were ninety-five adult male Brown-Norway rats (*Rattus norvegicus*; Charles River Laboratories Inc. Wilmington, MA). Seven rats were excluded from analysis due to poor injections or complications such as large vitreal hemorrhage or retinal detachment: anterograde colchicine experiment (n = 1), retrograde colchicine experiment (n = 5), anterograde rate experiment (n = 1). The remaining eighty-eight rats were used and analyzed as follows; development of the anterograde axonal transport assay technique (n = 8), development of the retrograde axonal transport assay technique (n = 6), anterograde CTB assay with colchicine experiment (n = 10), bilateral CTB controls for anterograde colchicine experiment (n = 4), retrograde CTB assay with colchicine experiment (n = 5), bilateral CTB controls for retrograde colchicine experiment (n = 10), rate of anterograde axonal transport (n = 26), rate of retrograde axonal transport (n = 10), naïve controls for rate experiments (n = 5), retrograde transport of latex microspheres (n = 2), retrograde transport of carbocyanine dye (n = 2). Rats were maintained under a 12-hour light/12-hour dark cycle with normal rat chow and water available ad libitum. The rats ranged in weight from 174 to 360 g and were 8 to 20 weeks old. All experimental methods and animal care procedures adhered to the Guide for the Care and Use of Laboratory Animals and were approved and monitored by the Institutional Animal Care and Use Committee at Legacy Health.

2.2. Anesthesia

For imaging and intravitreal injection procedures, animals were anesthetized with an intramuscular injection of a rodent cocktail containing ketamine (55 mg/kg, Ketaset; Fort Dodge Animal Health, Fort Dodge, IA), xylazine (5 mg/kg, AnaSed; Lloyd, Inc., Shenandoah, IA), and acepromazine maleate (1 mg/kg; Vedco, Inc., St. Joseph, MO). For

#178418 - $15.00 USD Received 19 Nov 2012; revised 10 Jan 2013; accepted 28 Jan 2013; published 30 Jan 2013

stereotactic injection procedures, animals were anesthetized with 2% isofluorane gas at 2 ml/min in 2:1 N_2O:O_2.

2.3. Imaging protocol

Rats were placed on a custom-built imaging stage and kept warm with a thermostatically controlled system (TP650; Gaymar Industries, Inc., Orchard Park, NY). Proparacaine hydrochloride (0.5%; Alcon Laboratories Inc., Fort Worth, TX) was instilled for topical anesthesia, and tropicamide (0.5%; Alcon Laboratories Inc.) and phenylephrine (2.5%; Bausch and Lomb Pharmaceuticals Inc., Tampa, FL) for topical mydriasis. Custom rigid gas-permeable contact lenses (3.5 mm posterior radius of curvature, 5.0 mm optical zone diameter, and +5.0 diopter back vertex power) were used to maintain corneal hydration and clarity. CSLO images of *in vivo* retina and post-mortem brain structures were obtained (Spectralis HRA + OCT; Heidelberg Engineering GmbH, Heidelberg, Germany) with an additional +25 diopter lens mounted to the camera objective. The infrared and BluePeak™ blue laser (488 nm) autofluorescence imaging modes (standard contrast settings) were used with 100 images averaged using the automatic real-time (ART) eye tracking software.

2.4. Development of the anterograde axonal transport assay

The anterograde transport assay was performed with a 2 µl intravitreal injection of 1% cholera toxin b-subunit conjugated to AlexaFluor488 (CTB; Molecular Probes C22841) dissolved in sterile PBS. In development of the assay, four animals had 5 µl intravitreal injections of 1% CTB, and one animal had 2 µl intravitreal injections of 0.5% CTB. Antibiotic ointment (neomycin, polymyxin B sulfates and dexamethasone, Falcon Pharmaceuticals Ltd, Fort Worth, Texas) was applied topically after injections. Animals were sacrificed at time points varying from 2 h to 34 days after intravitreal injection to determine the success and approximate time course of CTB transport to the optic nerve and superior colliculus. *In vivo* retinal imaging by CSLO was performed longitudinally at various time points (for up to 34 days after CTB injection) prior to sacrifice to confirm successful injection and uptake of CTB by RGCs. Animals were overdosed with pentobarbital sodium and phenytoin sodium (intraperitoneal 0.7–1.4 ml/kg; Euthasol Solution, Virbac Animal Health Inc., Fort Worth, Texas). Subsequently, the eyes were enucleated and the animal transcardially perfused with 125 ml of cold 4% paraformaldehyde in 0.5 M phosphate buffer (PB, pH 7.35) following an intracardiac injection of 0.1 ml heparin sodium (10,000 USP Units/ml, APP Pharmaceuticals). The retinas were dissected and mounted in 4% paraformaldehyde in 0.5 M PB for immediate fluorescence microscopy. The brain was dissected from the skull with the pre-chiasmal optic nerves attached and the cortices were splayed apart at the midline to reveal the dorsal aspect of the midbrain for imaging the superior colliculi.

The brain was immersion fixed in 4% paraformaldehyde in 0.5 M PB for at least 30 minutes prior to CSLO imaging. The patency of axonal transport was assessed from both post-mortem CSLO and microscopy images of the optic nerves and the superior colliculi to compare these two methods. CSLO has the potential for providing faster results and a field size and depth better suited to the task of imaging the nerves and colliculi than microscopy, particularly if the latter involves tissue blocking, cutting and imaging of serial sections. The CSLO images were obtained by positioning the brain on a custom-made mount strapped onto the stage. After CSLO imaging, the optic nerves and superior colliculi were dissected from the brain and mounted on a slide in phosphate buffer solution (PBS). Micrographs of the retinal flat-mounts (5x, 10x, 20x or 40x air objective), the ventral surface of the optic nerves (5x air objective) and the superior colliculi dorsal surface (5x air objective) were taken using a digital camera (QImaging Retiga 1300, Canada), mounted onto either a DMRXE or a DMLB microscope (Leica, Germany). Images in a single plane of best-focus were acquired with filter set #513808 (FITC; 450–490 nm excitation, 515 nm long pass emission; Chroma) for all specimens.

#178418 - $15.00 USD Received 19 Nov 2012; revised 10 Jan 2013; accepted 28 Jan 2013; published 30 Jan 2013

2.5. Development of the retrograde axonal transport assay

The retrograde transport assay was performed with 2 µl stereotactic injections of 1% CTB into both superior colliculi. The rat was affixed into a stereotactic frame (Kopf Instruments, CA), and then the head was shaved and sterilized with povidone-iodine prior to performing a 1.5 mm midline incision. The head tilt was adjusted so that the skull landmarks lambda and bregma were level. Bilateral holes were drilled through the skull using a Dremel bit and a Hamilton syringe was used to inject the CTB centered at co-ordinates corresponding to the center of each superior colliculus. The co-ordinates were optimized during development of the retrograde assay for successful CTB injection in Brown-Norway rats of this age and weight range (Table 1) and determined to be: −5.5 mm anterior-posterior (AP; relative to bregma), ±1.25 mm medial-lateral (ML), and −4.5, −4.25, −4.0, and −3.75 mm dorsal-ventral (DV; from the skull surface). At each of these four dorsal-ventral locations 0.5 µl of CTB was injected, with each injection made over the course of 30 seconds and a 30 second delay prior to moving the cannula to the next location. The cannula was slowly removed from the brain five minutes after the final injection. The incision was sutured or stapled closed, and buprenorphine (0.3 mg/ml) analgesic administered intra-muscularly.

Retinas were imaged *in vivo* by CSLO for up to 5 hours immediately after CTB injection and/or at longer post-injection time points of 1 to 68 days to determine the success of transport and time course of CTB fluorescence (Table 1). As described in the anterograde protocol, rats were sacrificed by transcardial perfusion at different time points (3 h to 68 days; Table 1), the retinas and brains were dissected, and post-mortem retinal micrographs and CSLO fluorescence images of the superior colliculus were taken to confirm injection success.

Table 1. Retrograde assay CSLO, microscopy and stereotactic surgery details

Rat ID	*In vivo* retinal CSLO time points (h)	Microscopy time point	Stereotactic co-ordinates (mm) AP, ML from Bregma; DV from skull
R025	1, 3, 3.5, 25, 48, 120 h, & 11, 49, 68 days	68 days	AP: −5.5, ML ± 1.5, DV −3.75
R062	32, 52	72 h	AP: −5.5, ML ± 1.5, DV −3.75
R065	28, 50	70 h	AP: −5.5, ML ± 1.5, DV −3.75
R066	28, 51	72 h	AP: −5.5, ML ± 1.5, DV −3.75
R068	29, 55.5	72 h	AP: −5.5, ML ± 1.5, DV −3.75
R070	27.5, 49	75 h	AP: −5.5, ML ± 1.5, DV −3.75
R073	26.5	28 h	AP: −5.5, ML ± 1.5, DV −4.5
R075	24	25 h	AP: −5.5, ML ± 1.5, DV −4.5
R076	25	26.5 h	AP: −5.5, ML ± 1.5, DV −4.5
R077	22.5	24 h	AP: −5.5, ML ± 1.5, DV −4.5
R078	24	25.5 h	AP: −5.5, ML ± 1.5, DV −4.5
R085	25	26 h	AP: −5.5, ML ± 1.25, DV −4.5 to −3.75
R086	24	25 h	AP: −5.5, ML ± 1.25, DV −4.5 to −3.75
R091	24	24 h	AP: −5.5, ML ± 1.25, DV −4.5 to −3.75
R097	1, 1.5, 2, 2.5, 3, 3.5, 4	4 h	AP: −5.5, ML ± 1.25, DV −4.5 to −3.75
R098	2, 2.5, 3, 3.5	3.5 h	AP: −5.5, ML ± 1.25, DV −4.5 to −3.75
R099	4, 6, 24	24.5 h	AP: −5.5, ML ± 1.25, DV −4.5 to −3.75
R110	23.5	24 h	AP: −5.5, ML ± 1.25, DV −4.5 to −3.75
R111	2.25, 2.75, 3, 3.5, 4, 4.5, 5	5 h	AP: −5.5, ML ± 1.25, DV −4.5 to −3.75
R113	2, 2.5, 3, 3.5, 4	4 h	AP: −5.5, ML ± 1.25, DV −4.5 to −3.75
R123	2.5, 3, 3.5, 4	4 h	AP: −5.5, ML ± 1.25, DV −4.5 to −3.75
R124	2.5, 3, 3.5, 4	4 h	AP: −5.5, ML ± 1.25, DV −4.5 to −3.75
R125	2, 2.5, 3, 3.5	3.5 h	AP: −5.5, ML ± 1.25, DV −4.5 to −3.75
R126	2.5, 3, 3.5	3.5 h	AP: −5.5, ML ± 1.25, DV −4.5 to −3.75
R129	2.5, 3	3.5 h	AP: −5.5, ML ± 1.25, DV −4.5 to −3.75
R130	2, 2.5, 3	3 h	AP: −5.5, ML ± 1.25, DV −4.5 to −3.75
R131	24	24 h	AP: −5.5, ML ± 1.25, DV −4.5 to −3.75

#178418 - $15.00 USD Received 19 Nov 2012; revised 10 Jan 2013; accepted 28 Jan 2013; published 30 Jan 2013

The bilateral retrograde assay of axonal transport was also tested using markers alternative to CTB, namely latex microspheres (size range 0.05–0.2 μm diameter, green retrobeads IX, Lumafluor) and the carbocyanine dye 3-octadecyl-2-[3-(3-octadecyl-2(3H)-benzoxazolylidene)-1-propenyl] (Di-O, Vybrant DiO cell-labeling solution, #V22886, Invitrogen). After injection (2 μl injection volume), retinas were imaged with *in vivo* CSLO for follow up periods of 3 to 15 weeks.

2.6. Colchicine protocol

To assess the dependence of anterograde transport on intact microtubules, animals had an intravitreal injection of colchicine (vitreal concentration 1.0 mM) in one eye and vehicle control in the fellow eye, followed by bilateral intravitreal injections of CTB between 2 – 4.5 hours later. The vehicle control was dimethyl sulphoxide (DMSO) in three animals and was deionized water passed through a 0.2 μm filter (#PN4192, Acrodisc syringe filter, Pall Life Sciences) in the remaining seven. Bilateral control animals had intravitreal CTB but not colchicine injections. Retinas were imaged *in vivo* by CSLO for up to 4 hours immediately after intravitreal injection of CTB and again at 24 hours, to assess uptake of CTB by the RGCs, and to confirm successful injections. Animals were sacrificed 24 hours after CTB injection for post mortem CSLO of the optic nerves and superior colliculi, and microscopy of retinal flat-mounts, as described above. The fluorescence intensity of the right and left optic nerves and superior colliculi was compared to determine whether CTB had reached these structures by anterograde axonal transport.

To assess the dependence of retrograde transport on microtubules, an intravitreal injection of colchicine (1.0 mM) was performed in one eye and a vehicle injection (all deionized water passed through a 0.2 μm filter) was given in the fellow eye, followed by bilateral stereotactic injections of CTB into the superior colliculi 2–2.75 hours later. Bilateral control animals had the CTB injections into the superior colliculi only. Retinas were imaged *in vivo* by CSLO at 24 hours after CTB injection into the superior colliculi. All animals were sacrificed at 24 hours for post mortem CSLO of the superior colliculi, and microscopy of retinal flat-mounts as described above. Successful superior colliculi injections for this purpose were defined as requiring both the central 10% of the superior colliculus surface filled by CTB, and an indication from CSLO retinal imaging that CTB had reached the optic disc (positive disc fluorescence).

2.7. Rate of anterograde axonal transport

The rate of anterograde transport of CTB was calculated based on the time taken for the CTB to travel from the retina to the superior colliculus. The rat visual pathway length (eye to superior colliculus) was measured at 19.9 ± 0.5 mm (n = 24 eyes) with calipers (including optic nerve stump, pre-chiasmal optic nerve, chiasm, and optic nerve tract to the middle of the superior colliculus). The time taken to first detect fluorescence in the optic nerve and the superior colliculus after intravitreal injection of CTB was quantitatively measured (as described below) to allow calculation of the bulk rate of transport (mm per day).

Three to four animals were sacrificed at each time point of 2, 3, 4, 5, 6, 7, 24 and 48 hours after successful unilateral intravitreal CTB injection (anterograde assay). Five animals were additionally sacrificed as naïve animals without injection of CTB or vehicle, two of which had no CSLO imaging to provide absolute naïve controls for microscopy, while the remaining three had CSLO imaging prior to microscopy.

CSLO images of the optic nerves and the superior colliculi and corresponding microscopy images underwent quantitative analysis of CTB fluorescence intensity using ImageJ software (NIH). For the optic nerve CSLO data, six square bins of size 75x75 pixels (120x120μm) positioned with equal spacing along each nerve and at the same locations between right and left, were measured for fluorescence intensity in arbitrary units (0 = black, 255 = white). For the optic nerve microscopy data, eleven square bins of size 150x150 pixels (320x320μm)

#178418 - $15.00 USD Received 19 Nov 2012; revised 10 Jan 2013; accepted 28 Jan 2013; published 30 Jan 2013

were similarly measured for fluorescence intensity. The normalized percent difference between the experimental and control eyes (for each bin position and in total for each time point) were determined for both the CSLO and the microscopy data. By normalizing the signal to the control, we control for autofluorescence. For the superior colliculi data, the right and left superior colliculi were outlined with the same "D" shaped polygon (matching the shape of each colliculus), the average fluorescence intensity at the surface was measured and the mean normalized difference between experimental and control superior colliculi determined for each time point. Note that in rat, approximately 95% of axons cross at the chiasm [39,60–62], so the experimental superior colliculus is of opposite laterality to the experimental pre-chiasmal optic nerve and eye.

2.8. Rate of retrograde axonal transport

The retrograde transport rate was determined from the time taken for CTB to first reach the eye after injection into the superior colliculus. Ten animals were imaged with fluorescent CSLO every 30 minutes for up to 5 hours after bilateral CTB injections into the superior colliculi (retrograde assay) to note the time taken to first detect fluorescence *in vivo* in the optic disc and retina (see Table 1 for precise imaging times). Since the length of the rat visual pathway is known, the rate of transport (mm per day) can be calculated. To obtain post-mortem microscopy results, rats were sacrificed at various time points between 3 and 5 hours after injections (Table 1). The three naive animals that had retinal CSLO and microscopy performed for the anterograde rate calculation were also used as naïve controls for the retrograde rate experiment. For this retrograde bulk rate experiment, successful injections required at least the central 30% of the superior colliculus surface filled by CTB on post-mortem CSLO imaging. This criterion was stricter than for the colchicine retrograde protocol because it involved fluorescence detection at threshold, rather than at supra-threshold.

2.9. Statistical analysis

For the effect of colchicine on anterograde transport, fluorescence intensity of the superior colliculus was assessed by analysis of variance (ANOVA) with Bonferroni-corrected post hoc comparisons across experimental groups. For the effect of colchicine on retrograde transport, the density of CTB–positive fluorescent RGCs was assessed by ANOVA with Bonferroni-corrected post hoc comparisons across experimental groups. To determine the time point that showed the first departure from background fluorescence, two separate approaches were undertaken: 1) one-sample t-tests with a theoretical mean of zero were applied to each post-injection time point and 2) the aggregate data for relative fluorescence intensity versus time after intravitreal CTB injection was fit using nonlinear regression to determine the time of departure from baseline (no relative fluorescence difference; see details and equation below). To compare CSLO and microscopy methods of measuring relative fluorescence intensity of the superior colliculus, nonparametric Spearman's correlations were performed. Statistics were calculated using Prism software (Version 5, GraphPad Software, Inc., La Jolla, CA).

3. Results

3.1. Anterograde axonal transport assay

Intravitreal CTB injection resulted in rapid uptake and filling of retinal nerve fiber layer (RNFL) axon bundles in normal eyes, typically beginning nearest the injection 15–20 min after injection and filling the entire fundus within 1–2 hrs. Figure 1 provides an example of longitudinal CSLO imaging *in vivo* after intravitreal CTB injection as well as comparison to *ex vivo* microscopy of the flat-mount retina. Fluorescent axon bundles were first visible by CSLO superiorly (nearest the injection site) within 10 minutes after the injection and filled most of the superior retina by 0.5 hours (Fig. 1(b)). By 24 hours (Figs. 1(c), 1(d)) the neuro-retinal rim of the optic disc fluoresced strongly; suggesting much of the CTB had entered the

#178418 - $15.00 USD Received 19 Nov 2012; revised 10 Jan 2013; accepted 28 Jan 2013; published 30 Jan 2013

nerve by this time. Retinal microscopy (Fig. 1(e)) confirmed uptake into the RGCs by revealing brightly fluorescent somas, as well as dendrites and proximal axons in most instances. With the epi-fluorescent microscope and CSLO, the somas are only visible in the regions between axon bundles since the axons also fluoresce strongly.

Figure 2 provides an example of post-mortem CSLO imaging and microscopy of the ventral and dorsal aspects of the midbrain 24 h after unilateral intravitreal CTB injection, which revealed a brightly fluorescent ipsilateral optic nerve through the chiasm, contralateral optic tract and contralateral superior colliculus after transport of CTB to these structures. The fellow control eye showed minimal auto-fluorescence of the retina, optic nerve, optic tract and superior colliculus. These results show that both CSLO and microscopy techniques are able to clearly detect successful anterograde transport of CTB to the superior colliculus.

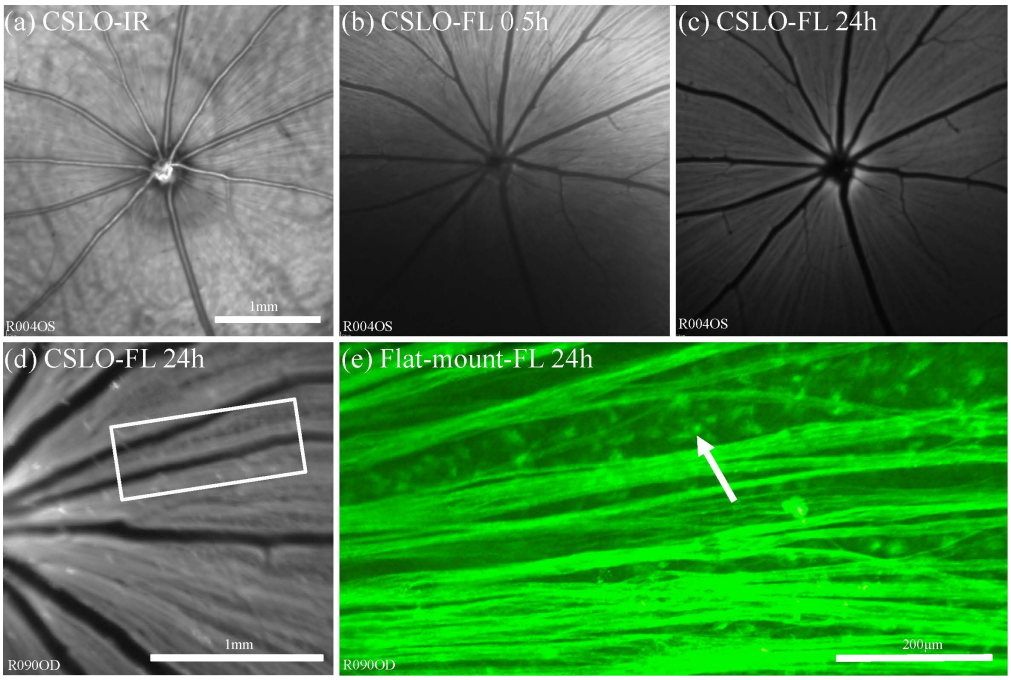

Fig. 1. Anterograde assay showing the time-course of CTB uptake into RGCs and their axons within the eye *in vivo* by CSLO. (a) CSLO infrared reflectance image ("CSLO-IR") provides orientation to the ocular fundus. (b)–(c) CSLO fluorescence ("CSLO-FL") images taken at 0.5 h (b), and 24 h (c) after intravitreal CTB injection demonstrate increasing uptake and transport of CTB in RGC axons over time. RGC uptake of CTB is first seen superiorly near the injection site; axon bundle filling typically progresses toward the optic disc and throughout the rest of the fundus. (d) High magnification CSLO-FL image obtained in a different eye 24 h after CTB injection and (e) flat-mount retinal microscopy (x20) corresponding to inset box in (d) demonstrate fluorescent RGC soma (arrow) and axons. Scale bar in (a) applies (a)–(c).

To evaluate the longer term time-course and persistence of CTB fluorescence in RGCs, one retina from one rat was imaged *in vivo* by CSLO immediately after intravitreal CTB injection, then subsequently at 1 day, 28 days, 32 days and 34 days follow up. At 24 hours the *in vivo* fluorescent CSLO image showed the usual pattern of CTB uptake with strong filling of ganglion cells and retinal nerve fiber bundles, in similar fashion to Figs. 1(c), 1(d) and Fig. 2(a). However, by 28 days the *in vivo* image had become more punctate, portraying individual RGCs only and no longer the nerve fiber bundles. By 34 days there was considerable depletion in the RGC numbers seen *in vivo*, indicating that CTB fades from RGCs at 1 month after intravitreal injection.

#178418 - $15.00 USD Received 19 Nov 2012; revised 10 Jan 2013; accepted 28 Jan 2013; published 30 Jan 2013

3.2. Retrograde axonal transport assay

Injection of CTB into the superior colliculi resulted in subsequent fluorescence of the contralateral optic discs observed *in vivo* by CSLO, followed by increasing accumulation of fluorescence within individual RGCs. Figure 3 shows results 24 hours after bilateral superior colliculus injections, when accumulation of CTB fluorescence is nearing its peak (time course results are shown in subsequent figures for experiments on transport rate). Figure 3 shows that RGC somas are more visible in the retrograde assay than in the anterograde assay, presumably due to a lower CTB concentration within the overlying intraretinal axons. Baseline CSLO of retinas *in vivo* prior to superior colliculi CTB injection shows weak auto-fluorescence of the retina depending on the CSLO sensitivity used during image acquisition (i.e., Figure 2(c)). Post-mortem CSLO of the superior colliculi (Fig. 3(g)) shows CTB usually diffuses well throughout the colliculi, although often not completely, and allows confirmation of a successful injection. The extent of CTB diffusion through the superior colliculi seems to correlate reasonably with the extent of retinal area with positive ganglion cell fluorescence, as would be expected since visual space is represented topographically in the superior colliculus [63].

To evaluate the extended time-course of CTB fluorescence in RGCs, the retinas of one rat were imaged by CSLO *in vivo* immediately after bilateral superior colliculi CTB injections, then subsequently at 1, 2, 5, 11, 49 and 68 days follow up. By 24 hours the label showed good

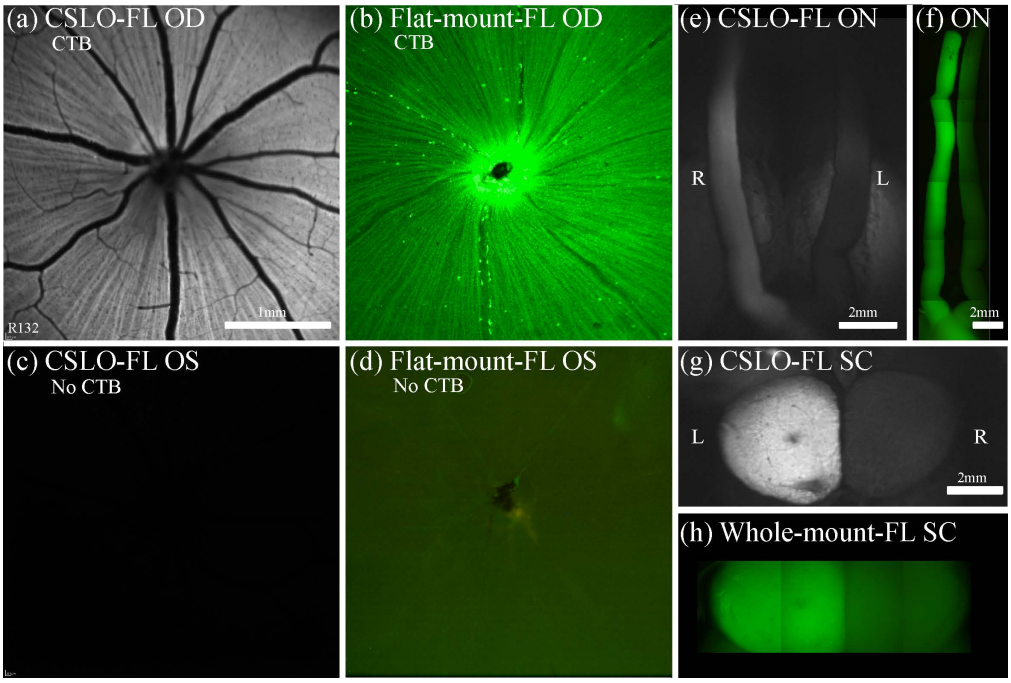

Fig. 2. Results of anterograde axonal transport 24 h after unilateral CTB injection. The right eye (a), (b) received an intravitreal injection of CTB, while the left eye (c), (d) was a non-injected control. CSLO images *in vivo* (a), (c) and post-mortem micrographs (x5) of flat-mount retina (b), (d) show strong CTB fluorescence in RGCs and axons of the right eye only. Post-mortem imaging of the optic nerves and chiasm (ventral view, (e), (f) and superior colliculi (dorsal view, (g), (h)) obtained either by CSLO (e), (g) or by epi-fluorescence microscopy (x5) montages (f), (h) show unilateral fluorescence of the ipsilateral optic nerve and contralateral superior colliculus. This indicates that CSLO and microscopy are both able to clearly detect successfully transported CTB to the optic nerves and superior colliculi. Scale bars: (a) applies (a)–(d); (g) applies (g), (h). Abbreviations: fluorescence (FL), right eye (OD), left eye (OS), right (R), left (L), optic nerves (ON), superior colliculi (SC).

#178418 - $15.00 USD Received 19 Nov 2012; revised 10 Jan 2013; accepted 28 Jan 2013; published 30 Jan 2013

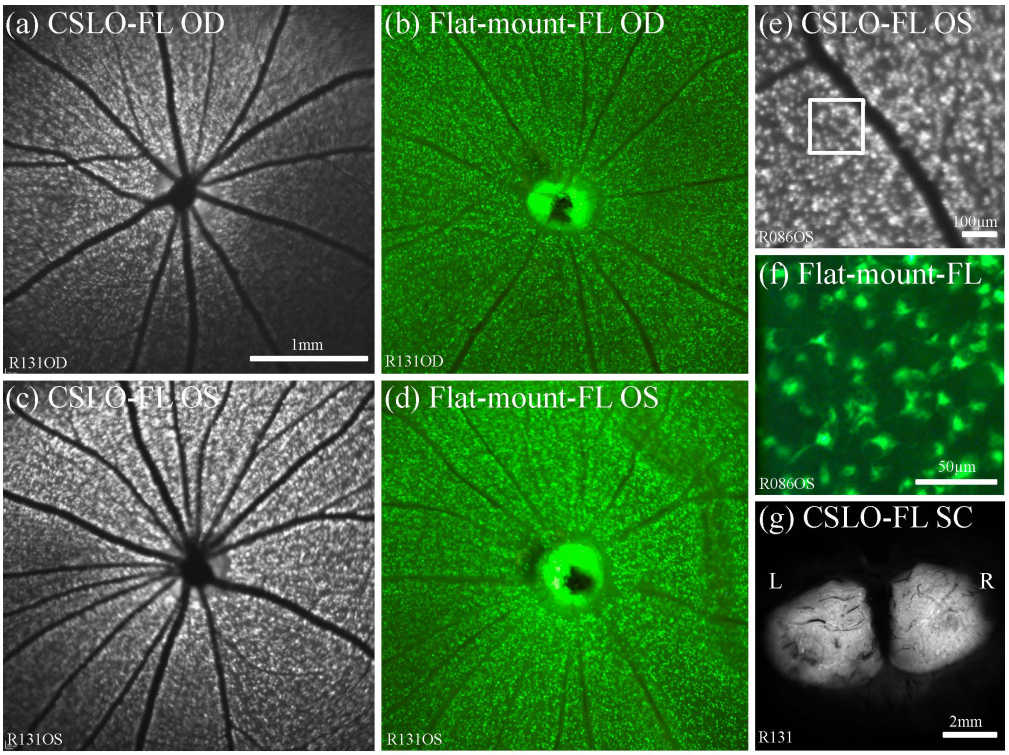

Fig. 3. Results of retrograde axonal transport 24 h after CTB injection bilaterally into the superior colliculi. (a)–(d) CSLO fundus images *in vivo* and post-mortem micrographs (x5) of flat-mount retinas from the right and left eyes demonstrate strong CTB fluorescence of RGC somas and optic discs bilaterally, indicating successful axonal transport of CTB. Higher magnification CSLO fundus image *in vivo* (e) and post-mortem microscopy (x20) of the retina (f) shows the fluorescent RGC somas and dendrites. Box in (e) indicates region shown in (f). Post-mortem imaging of the dorsal midbrain by CSLO (g) reveals bilateral fluorescence of both superior colliculi indicating that CTB diffuses throughout the superior colliculi from the central injection sites. Scale bars: (a) applies (a)–(d). Abbreviations: fluorescence (FL), right eye (OD), left eye (OS), right (R), left (L), optic nerves (ON), superior colliculi (SC).

coverage across the RGCs in the central retina of both eyes, and the fluorescence intensity and coverage was maintained over the first 11 days. By 49 days the number of fluorescent RGCs seen *in vivo* had declined dramatically and by 68 days there was only a small group of cells still visible near the optic disc. This indicates that CTB fluorescence after superior colliculus injection fades from RGCs by 2 months.

Since both the anterograde and retrograde assays produced an unequivocally strong CTB fluorescence at their targets by 24 hours, we chose this as the assay time-point for the following retrograde assay experiments with colchicine.

3.3. Effect of colchicine on anterograde and retrograde transport of CTB

Unilateral pre-treatment with colchicine (by intravitreal injection) resulted in profound inhibition of anterograde axonal transport of CTB from the colchicine-injected eye. Figure 4 demonstrates the effect in one representative example. The results for a representative bilateral positive control are shown in the left pair of columns demonstrating brightly fluorescent axons within the RNFL of both eyes (Figs. 4(a), 4(b), 4(e), 4(f))) and symmetrically bright fluorescence of the optic nerves, chiasm and tracts (Fig. 4(i)) and superior colliculi (Fig. 4(j)) 24 hours after bilateral intravitreal CTB injections. In contrast, the right pair of columns shows the results for an animal pre-treated with a unilateral colchicine

#178418 - $15.00 USD Received 19 Nov 2012; revised 10 Jan 2013; accepted 28 Jan 2013; published 30 Jan 2013

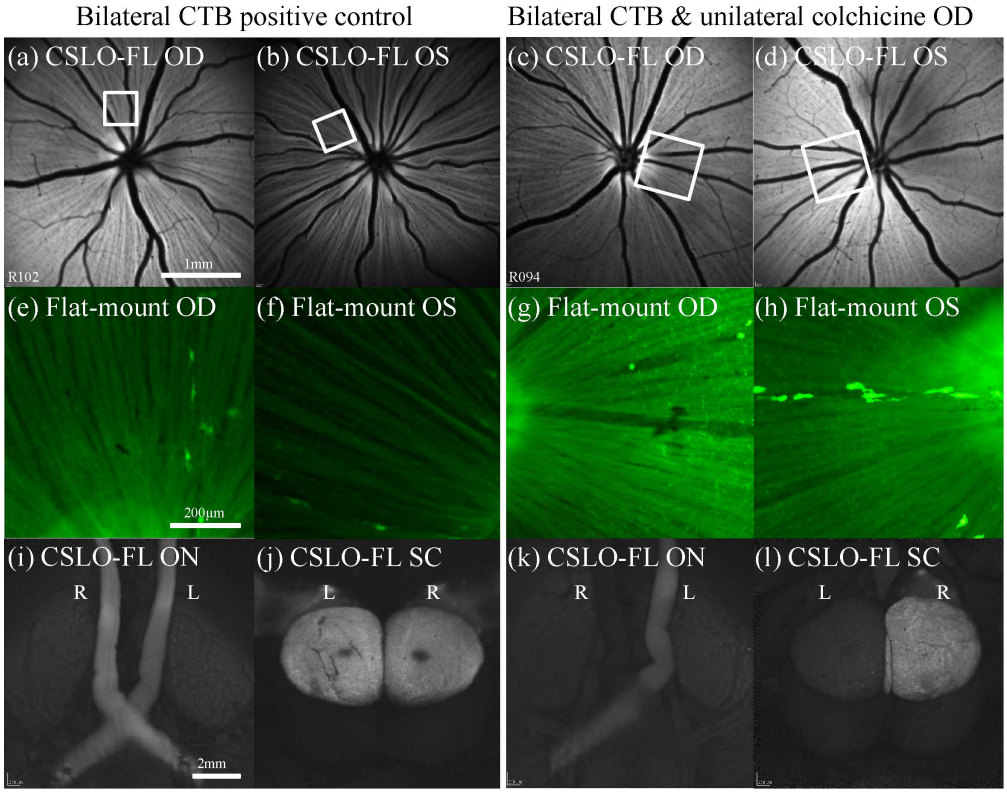

Fig. 4. Effect of colchicine on anterograde axonal transport. (a)–(d) Fluorescence mode CSLO fundus images obtained *in vivo* 24 h after CTB injections from the right and left eyes of a bilateral CTB positive control rat (a), (b) and another bilateral CTB rat that had unilateral (OD) pre-treatment with intravitreal colchicine (c), (d). (e)-(h) High magnification post-mortem fluorescence micrographs of flat-mount retinas from the bilateral positive control (x20; (e), (f)) and the unilateral colchicine animal (x10; (g), (h)). The CSLO images and the micrographs demonstrate strong CTB fluorescence of RGC somas, RNFL and optic discs bilaterally, indicating successful uptake of CTB by RGCs across all retinas. Box in (a)–(d) indicates region shown in (e)–(h). Post-mortem imaging of the ventral and dorsal midbrain by CSLO (i)–(l) reveals bilateral fluorescence of both optic nerves and tracts (i) and both superior colliculi (j) in the bilateral positive control rat, indicating patent axonal transport of CTB in both pathways. However for the unilateral colchicine rat, the ipsilateral optic nerve and contralateral optic tract (k) and contralateral superior colliculus (l) to the colchicine-injected eye exhibit minimal fluorescence, indicating disruption of axonal transport in the colchicine-treated pathway. The fellow control eye (OS) in the unilateral colchicine rat shows patent axonal transport (CTB fluorescence) at its corresponding brain structures (k), (l). Scale bars: (a) applies (a)–(d), (e) applies (e)–(h), (i) applies (i)–(l). Abbreviations: fluorescence (FL), right eye (OD), left eye (OS), right (R), left (L), optic nerves (ON), superior colliculi (SC).

injection (1.0 mM) 2 hours prior to bilateral intravitreal CTB injection, demonstrating weak-to-no fluorescence of the ipsilateral optic nerve, chiasm and contralateral optic tract (Fig. 4(k)) and colliculus (Fig. 4(l)). Interestingly, the axons within the colchicine-treated eye (OD, Fig. 4(c)) exhibit essentially normal CTB fluorescence, evident both *in vivo* by CSLO (Figs. 4(a)–(4d)) and post mortem by microscopy of flat-mount retinae (Figs. 4(e)–4(h)), suggesting that CTB uptake occurs all along the axons, not strictly at the RGC soma. The effect of colchicine to severely disrupt anterograde axonal transport was unequivocal for all rats in this experiment (n = 10).

Figure 5 shows the results of the effect of colchicine on anterograde axonal transport of CTB: colchicine reduced the fluorescence intensity of the contralateral superior colliculus to the level of non-injected controls (CTB–). Contrast between hemispheres was nearly as great

#178418 - $15.00 USD Received 19 Nov 2012; revised 10 Jan 2013; accepted 28 Jan 2013; published 30 Jan 2013

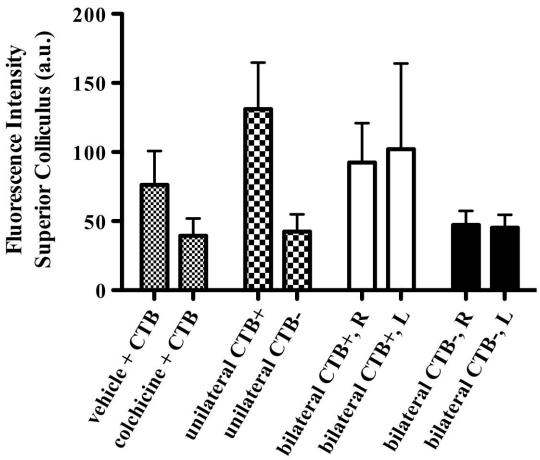

Fig. 5. Effect of colchicine on anterograde axonal transport. Average fluorescence intensity (±SEM) is shown for the group of rats (n = 7, bars with small checks) in which one eye was pre-treated with an intravitreal injection of either vehicle or colchicine prior to intravitreal injection of CTB; a unilateral control group of rats (n = 3, bars with larger checks) in which the intravitreal injection of CTB was unilateral with the fellow eye serving as a non-injected control (CTB–); a bilateral positive control group of rats (n = 4, open bars) in which CTB was injected into the vitreous bilaterally (CTB+)); and a negative control group of naïve rats (n = 3, solid bars) which were sacrificed without any CTB injection in either eye (CTB–). Colchicine reduced the fluorescence intensity of the contralateral superior colliculus 24 h after CTB injection to the level of non-injected controls (CTB–); contrast between hemispheres was nearly as great as that in the group of unilateral controls. Abbreviations: right superior colliculus (R) and left superior colliculus (L).

as that in the group of unilateral controls: fluorescence of the superior colliculi contralateral to the eyes pre-treated with colchicine was significantly reduced compared with the group of fellow controls pre-treated with vehicle ($p < 0.05$) or to the groups of unilateral or bilateral positive controls ($p < 0.05$). Unilateral colchicine did not appear to significantly alter CTB transport in the fellow control (vehicle-injected) eyes: there were no significant differences between the superior colliculi contralateral to the eyes pre-treated with vehicle versus those of either the bilateral control group or the unilateral control groups.

Retrograde transport of CTB was also severely disrupted (and/or delayed) by pre-treatment with intravitreal colchicine in all animals studied. Figure 6 demonstrates the results for one representative example. In the eye pre-treated with intravitreal colchicine injection (Figs. 6(a), 6(b)), there was only patchy or weak fluorescence of RGCs 24 hours after bilateral CTB injections to the superior colliculi, as compared to the vehicle-injected control fellow eye (Figs. 6(c), 6(d)) or to bilateral positive controls such as that shown in Fig. 3. This result was unequivocal in all five animals. In all colchicine eyes, retrograde CTB reached the optic disc, perhaps reflecting a more limited effect of colchicine along the distal optic nerve and tract over this relatively short post-injection duration. Importantly, the success of the superior colliculus injections can be confirmed rapidly and effectively by post mortem CSLO imaging of the dorsal midbrain (Figs. 6(e), 6(f)), ruling-out the possibility of injection failure as a potential cause of apparent transport deficit.

Figure 7 shows the results for all five eyes included to evaluate the effect of colchicine on retrograde axonal transport of CTB. Colchicine markedly reduced the density of CTB positive RGCs as compared to either the group of fellow (vehicle-treated) control eyes or to either group of bilateral positive control eyes ($p < 0.05$). Though there was no significant difference between colchicine-treated eyes and negative controls ($p > 0.05$), RGC density was not reduced to zero in colchicine-treated eyes indicating that retrograde transport was not completely suppressed by this pre-treatment with intravitreal colchicine. The colchicine effect was clear whether RGC density was measured *in vivo* by CSLO (Fig. 7(a)) or post mortem by

#178418 - $15.00 USD Received 19 Nov 2012; revised 10 Jan 2013; accepted 28 Jan 2013; published 30 Jan 2013

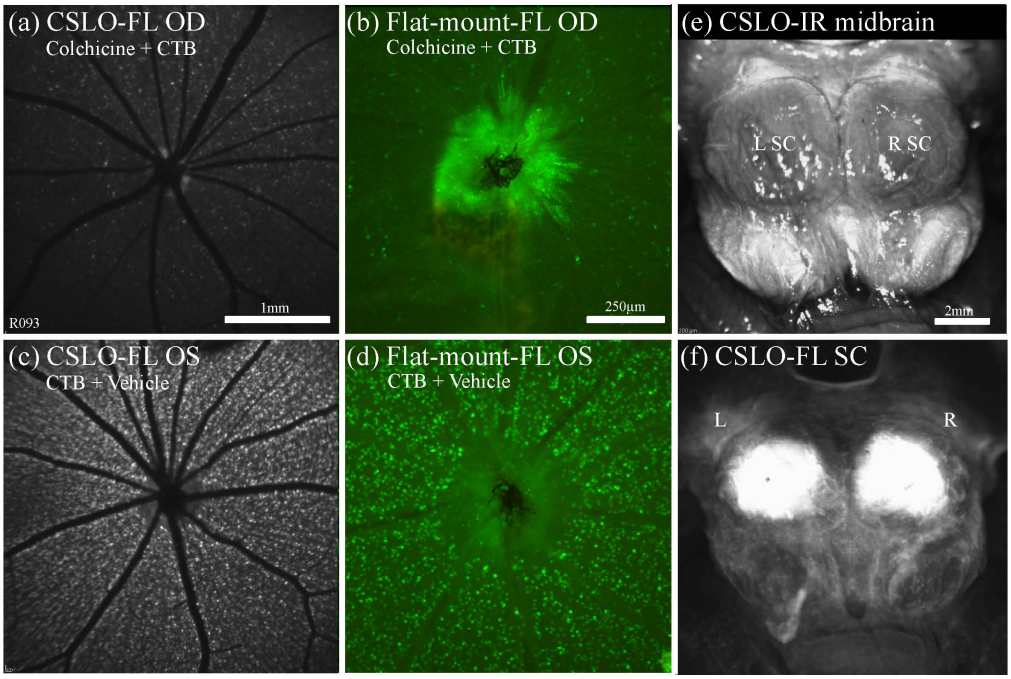

Fig. 6. Effect of colchicine on retrograde axonal transport. (a)–(d) CSLO fluorescence fundus images *in vivo* of the right (a) and left (c) eyes and post-mortem micrographs (x10) of flat-mount right (b) and left (d) retinas, 24 h after bilateral superior colliculi injections of CTB and unilateral (OD) pre-treatment with intravitreal colchicine. There was substantially less CTB fluorescence in the RGCs of the eye pre-treated with colchicine (a), (b) than the fellow control eye (c), (d), indicating disruption of retrograde axonal transport of CTB in the colchicine eye only. The RGC fluorescence in the fellow control eye (c), (d) is similar to the that in the bilateral positive control shown in Fig. 3, indicating patent axonal transport of CTB. (e) CSLO infrared reflectance image provides orientation to the dorsal midbrain including the superior colliculi. (f) Accompanying CSLO in fluorescence mode shows that both superior colliculi fluoresce equally with near full coverage, indicating that the difference in RGC fluorescence is not due to a failed CTB injection. Scale bars: (a) applies (a), (c), (b) applies (b), (d), (e) applies (e), (f). Abbreviations: fluorescence (FL), right eye (OD), left eye (OS), right (R), left (L), infra-red (IR), superior colliculi (SC).

microscopy of retinal flat-mounts (Fig. 7(b)). There was a strong association between mean RGC density measured *in vivo* by CSLO and post-mortem by microscopy of retinal flat-mounts ($R^2 = 0.98$, $p < 0.0001$), though the former underestimated the latter by ~30% (slope = 0.68), which is apparent in the comparison between Figs. 7(a) and 7(b).

3.4. Rate of anterograde axonal transport

Figures 2 and 4 demonstrated strong fluorescence of the optic nerve, chiasm, tract and superior colliculus 24 hours after intravitreal injection of CTB. That the superior colliculus, approximately 20 mm from the globe, was already exhibiting strong fluorescence 24 hours after injection indicates that anterograde transport of CTB occurs at a minimum rate of 20 mm/day, which is ~3–4x faster than membranous diffusion such as in the case of carbocyanine dyes [59,64,65]. In order to further evaluate the rate of anterograde CTB transport we examined post-mortem fluorescence of these structures at earlier (2–7 h) post-injection time points. Figure 8 shows representative examples of midbrain CSLO imaging at time points 5, 6, and 7 hours after unilateral CTB injection, around the time that fluorescence was first unequivocally brighter along the ipsilateral optic nerve but only just beginning to exceed background noise and autofluorescence in the contralateral superior colliculus. Image analysis of post-mortem CSLO (Fig. 8) and microscopy (data not shown) reveal that relative

#178418 - $15.00 USD Received 19 Nov 2012; revised 10 Jan 2013; accepted 28 Jan 2013; published 30 Jan 2013

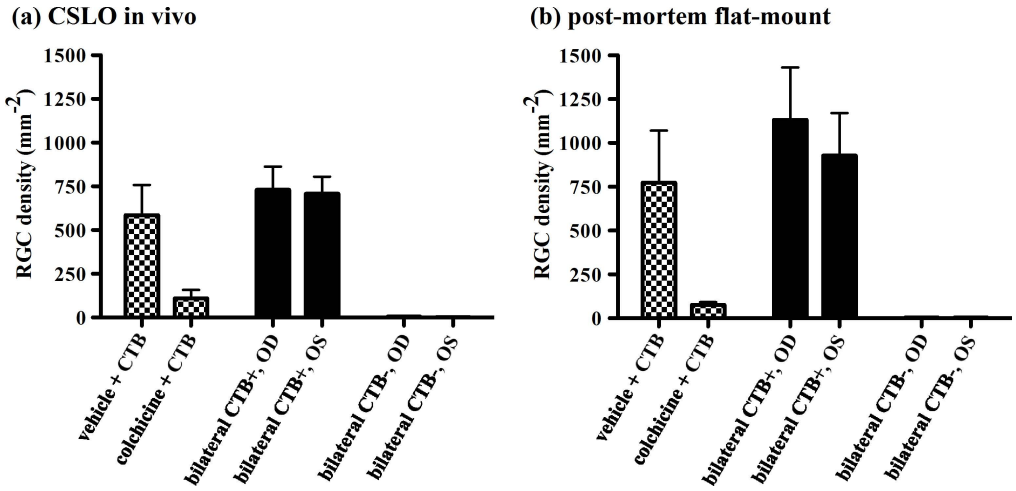

Fig. 7. Effect of colchicine on retrograde axonal transport. Average RGC density (±SEM) measured *in vivo* by CSLO (a) and post-mortem by microscopy of retinal flat-mounts (b) is shown for the group of rats (n = 5, bars with checks) in which one eye was pre-treated with an intravitreal injection of either vehicle or colchicine prior to bilateral injection of CTB into the superior colliculus; a bilateral positive control group of rats (n = 9, open bars) in which CTB was injected into the superior colliculus bilaterally (CTB+)); and a negative control group of naïve rats (n = 3, solid bars) which were sacrificed without any CTB injection (CTB–). Colchicine reduced the density of CTB–positive RGCs nearly completely (i.e., nearly to the level of non-injected controls). Abbreviations: right eye (OD) and left eye (OS).

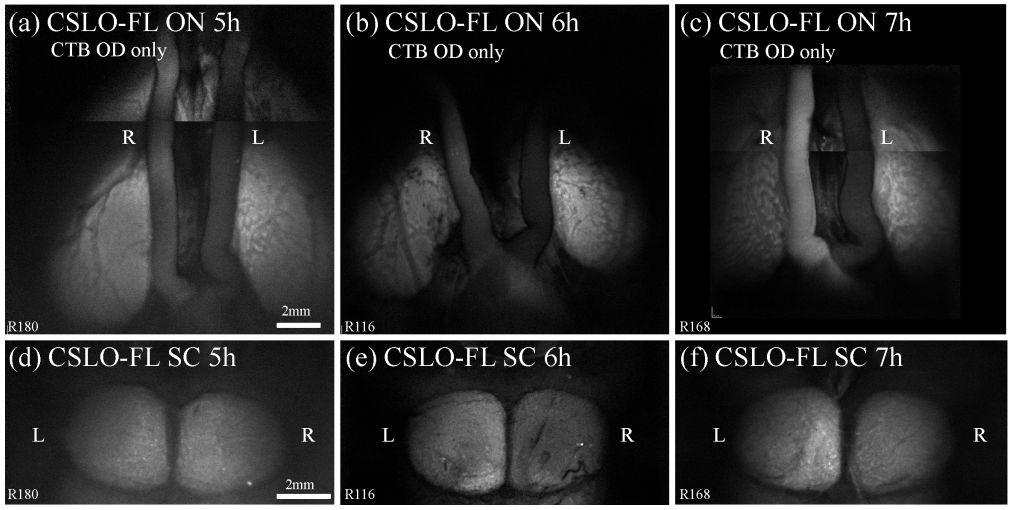

Fig. 8. Results of anterograde transport rate experiment. Representative examples from a cross-sectional series demonstrate the time of earliest detected CTB fluorescence at the optic nerves and superior colliculi after unilateral intravitreal CTB injections into the right eye. (a)–(c) Post-mortem imaging (montages) of the ventral midbrain by CSLO at (a) 5h, (b) 6h, and (c) 7h after CTB injection reveals greater fluorescence in the ipsilateral (right) optic nerve than the left, first noticeable at 5h (a) and more obviously noticeable at 6h (b) and 7h (c). (d)–(f) Post-mortem imaging of the corresponding dorsal midbrains by CSLO at (d) 5h, (e) 6h, and (f) 7h shows greater relative fluorescence intensity in the contralateral (left) superior colliculus, first noticeable at 6h (e) and more clearly noticeable by 7h (f). These results show that CTB reaches the optic nerve by 5h after intravitreal injection and the superior colliculus by 6h, indicating that CTB travels by fast active axonal transport when compared to known rates [1]. Scale bars: (a) applies (a)–(c), (d) applies (d)–(f). Abbreviations: fluorescence (FL), right eye (OD), right (R), left (L), optic nerves (ON), superior colliculi (SC).

#178418 - $15.00 USD Received 19 Nov 2012; revised 10 Jan 2013; accepted 28 Jan 2013; published 30 Jan 2013

differences in fluorescence intensity between experimental right and fellow control left optic nerves are first evident at 4–5 hours after CTB injection (e.g., Fig. 8(a)), while differences between experimental left and fellow control right superior colliculi are first evident 6 hours after injection (e.g., Fig. 8(e)).

Figure 9 shows the data for all animals and time points evaluated in this experiment by plotting relative fluorescence intensity (injected side relative to non-injected side) versus time after unilateral intravitreal injection. Figure 9 demonstrates that after a brief lag, relative fluorescence intensity begins to increase within the optic nerve (Fig. 9(a)) and superior colliculus (Fig. 9(b)) approaching a plateau at 48 hours. As expected, the lag is longer for the colliculus than the optic nerve. We followed two approaches for quantitative analysis of the early time point data series. First, we applied statistical analysis of each time point to determine when fluorescence was first detectable above the 'background' level in the ipsilateral optic nerve and contralateral superior colliculus (using a one sample t-test with a theoretical mean for comparison to zero). Though relative fluorescence of the ipsilateral optic nerve was already increasing at the earliest time point (2 hours, Fig. 9(a)) relative to naïve controls, it was first significantly greater than the contralateral optic nerve (non-injected eye) 4 hours after CTB injection ($p = 0.021$). Relative fluorescence of the contralateral superior colliculus was first significantly greater than the opposing side (ipsilateral superior colliculus) 6 hours after CTB injection ($p = 0.022$, Fig. 9(b)).

We also used the results of a nonlinear regression to determine the time that relative fluorescence intensity first began to increase above background (X_0). The potential advantage of this latter approach is to be unconstrained by the specific experimental time points chosen a priori for animal sacrifice. Using the equation $Y = IF(X < X_0, Y_0, Y_0 + (Plateau-Y_0)*(1 – exp(–K*(X – X_0))))$, the X_0 parameter was determined to be 1.6 hours after injection for the optic nerve and 5.5 hours for the superior colliculus. The results of the nonlinear regression are also shown in Fig. 9.

Thus, the two quantitative approaches provide a similar result of 5.5 to 6 hours to reach the superior colliculus (20 mm from the eye), so the estimate for the bulk rate of anterograde axonal transport of CTB is 80–90 mm/day.

The same analysis methods were applied to post-mortem preparations of optic nerve and superior colliculi and analyzed with microscopy (e.g., Figs. 2(f) and 2(h), respectively).

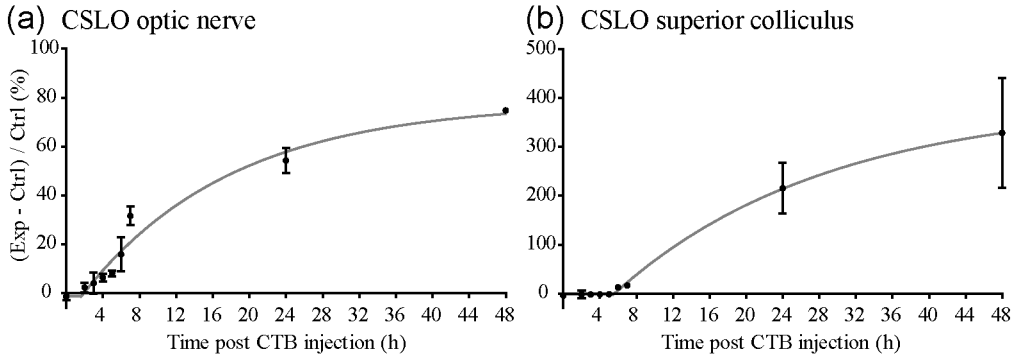

Fig. 9. Results of experiment to estimate bulk-rate of anterograde axonal CTB transport. Relative fluorescence intensity (CTB injected side (Exp) relative to non-injected (Ctrl) side) is plotted versus time after unilateral intravitreal CTB injection for the ipsilateral optic nerve (a) and contralateral superior colliculus (b). Solid line through data represents results of fit to the data of the equation: $Y = IF(X < X_0, Y_0, Y_0 + (Plateau – Y_0)*(1 – exp(–K*(X – X_0))))$, which was used as a secondary method to determine the first time after injection that fluorescence intensity began to rise above that of the opposite-side structure (i.e., the X_0 parameter corresponding to the point that exponential growth began from baseline). For optic nerve, $X_0 = 1.64$ (95% CI –0.07 to 3.35); for superior colliculus, $X_0 = 5.48$ (95% CI 2.78 to 8.19). Error bars = SEM. $N \geq 3$ rats per time point. Abbreviations: Exp = Experimental, Ctrl = Control.

#178418 - $15.00 USD Received 19 Nov 2012; revised 10 Jan 2013; accepted 28 Jan 2013; published 30 Jan 2013

Although the relative fluorescence intensity data obtained by CSLO and microscopy showed a good correlation for both the optic nerves (Spearman $r = 0.983$, $p < 0.001$) and superior colliculi (Spearman $r = 0.817$, $p = 0.011$), the sensitivity of the CSLO method was superior due to higher contrast and lower variance (data not shown).

3.5. Rate of retrograde axonal transport

Because CTB fluorescence within the eye can be evaluated *in vivo* by CSLO after retrograde transport from the superior colliculus, the experiment to estimate the bulk rate of retrograde axonal transport could be accomplished using longitudinal imaging (rather than by sacrificing groups of animals at specific time points such as in the previous experiment on anterograde transport rate). We imaged the ocular fundus by CSLO every 15–30 min after CTB injection into the superior colliculus. Figure 10 provides an overview of the results for one individual representative example. We found that the first sign of increased fluorescence (above background 'noise' and autofluorescence) typically occurred at the optic disc within 2.5 to 3.5 hours (in 17 out of 20 eyes, see, e.g., Figs. 10(b), 10(e)), representing a fast axonal transport rate of 136 to 191 mm per day (159 mm per day on average). Optic disc fluorescence might have been brighter than adjacent retinal nerve fiber bundle fluorescence because the axons (and their CTB concentration) are being viewed axially rather than transversely within the disc and because the background (autofluorescence) of the retinal pigment epithelium is stronger than that of the optic nerve head. Following optic disc fluorescence, individual RGCs generally begin to exhibit fluorescence above background 3 to 4 hours (Figs. 10(c), 10(f)) after CTB injection (in 15 of 20 eyes) and reach full coverage and brightness at 24 to 48 hours. Occasionally CTB fluorescence was detected in the RGC somas before the optic disc (in 3 out of 20 eyes), but given the relatively short amount of time between appearance at the optic disc and appearance in the retina (generally 0.5h), this variability may not be surprising; it depends on the degree of (radial) axon bundle filling for the fastest CTB transported as well as the relative image quality of the optic disc margin versus the surrounding retina.

Post-mortem microscopy of the retinal flat-mounts (Figs. 10(g), 10(h)) confirmed the results obtained *in vivo* by CSLO, with CTB fluorescence detected in all 20 eyes when compared to the six naïve control retinas. The retrograde injection was successful as judged by post-mortem CSLO imaging of the superior colliculi in all replicates (e.g., Fig. 10(i)), but with varying coverage and intensity, which probably contributed a degree of variability in the rate estimates.

3.6. Retrograde transport of latex microspheres and Di-O

To determine if microbeads or carbocyanine dye could serve as suitable alternatives for RGC labeling (and/or to be used in the axonal transport assay), bilateral injections of green retrobeads IX and Di-O dye into the superior colliculi were performed and the fundi were subsequently monitored *in vivo* by CSLO for retrograde transport. For both tracers, RGC fluorescence was much slower to accumulate (at least 3–4 times slower) as compared with CTB, though it also persisted longer than CTB, for up to 15 weeks. However, for both tracers only a limited region of the retina showed positive RGC fluorescence, and post-mortem CSLO of the superior colliculi revealed limited diffusion at the injection sites. This lack of diffusion away from the injection site has been previously reported in latex microbeads [66,67] and carbocyanine dyes [65]. The results indicate that microbeads and Di-O are not appropriate markers for the axon transport assay as transport is only able to be assessed for a small minority of RGC axons corresponding to the precise injection site rather than the majority of axons in the optic nerve, plus the transport rates are slower than for CTB. Given these results, we did not subsequently test colchicine dependence of either potential tracer.

#178418 - $15.00 USD Received 19 Nov 2012; revised 10 Jan 2013; accepted 28 Jan 2013; published 30 Jan 2013

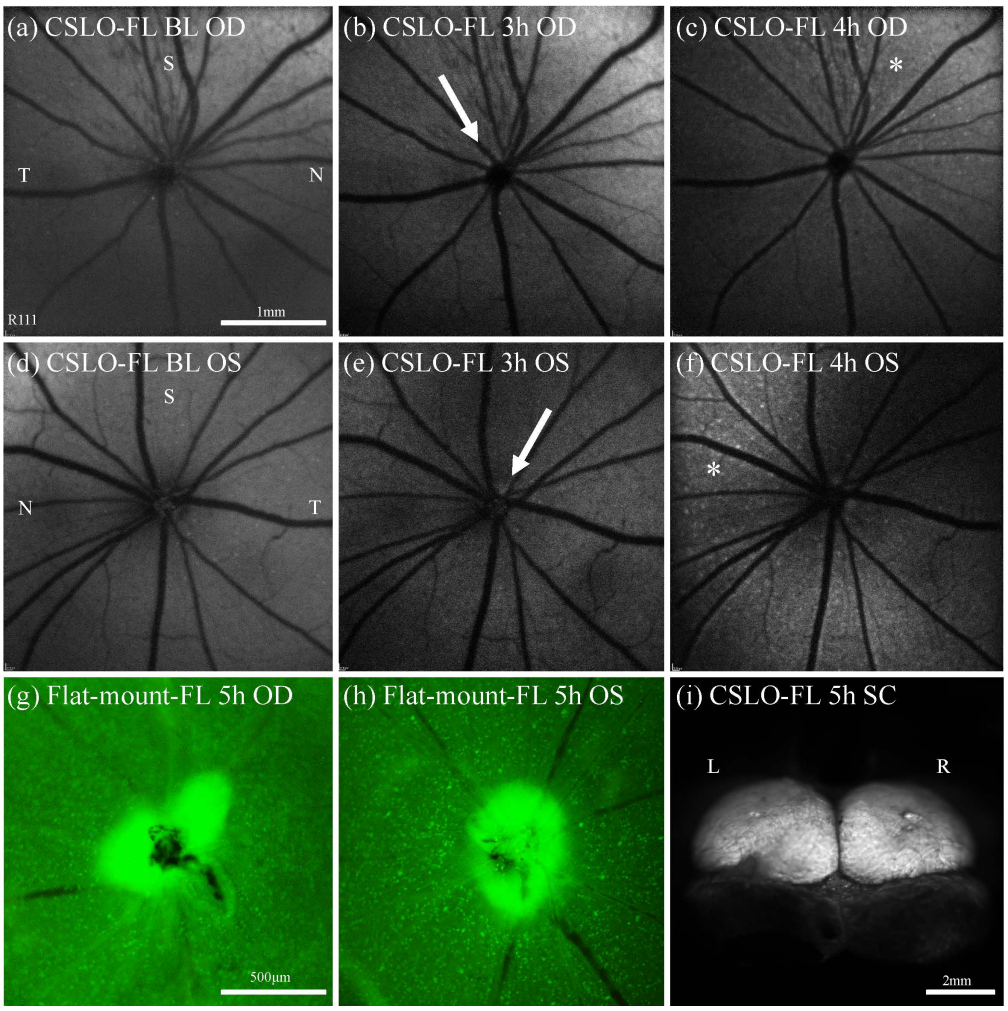

Fig. 10. Examples from a longitudinal series demonstrate the time of earliest detected CTB fluorescence at the optic disc and RGCs after bilateral superior colliculi CTB injections in order to determine the rate of retrograde transport of CTB. CSLO fluorescence fundus images (a)–(f) were taken *in vivo* at pre-injection baseline (a), (d) then every 30 min from 2 to 5 h after CTB injection. At 3h the first sign of optic disc fluorescence (arrow) was noted in the right (b) and left (e) eyes, clearly brighter than at baseline. At 4h the first sign of RGC fluorescence (asterisk) was noted predominantly superior-nasally in the right (c) and left (f) eyes. Post-mortem micrographs (x10) of flat-mount right (g) and left (h) retinas at 5h after injection confirm CTB fluorescence at the disc and RGCs in all retinal quadrants. Brightness and contrast of images were adjusted to maximize visibility in panels of this figure. Scale bars: (a) applies (a)–(f), (g) applies (g), (h).. Abbreviations: fluorescence (FL), right eye (OD), left eye (OS), superior (S), inferior (I), nasal (N), temporal (T).

4. Discussion

This study confirms CTB can be used as a highly sensitive neural tract tracer and demonstrates that its transport occurs by fast, active, microtubule-dependent mechanisms in the rat anterior visual pathway. Further, the results indicate that the patency of fast retrograde axonal transport can be monitored *in vivo* with fluorescence CSLO. CTB has often been used as a neural tract tracer [33–43,68–70] and recently has been used ostensibly to evaluate axonal transport in experimental models of optic nerve injury [27,71]. However, experiments to test the hypothesis that CTB moves by fast active axonal transport *in vivo* and is dependent on

#178418 - $15.00 USD Received 19 Nov 2012; revised 10 Jan 2013; accepted 28 Jan 2013; published 30 Jan 2013

intact microtubules per se, rather than moving by passive diffusion, have not previously been reported. In the present study, CTB transport shows sensitivity to colchicine, a known microtubule disruptor [48–50], and calculated bulk rates of CTB transport *in vivo* confirm that it travels along microtubules by a fast active mechanism in both anterograde and retrograde directions. Previous studies have reported varying rates of anterograde transport of CTB, differing from 6 to 8 mm over 1–3 days in cat [35], and 2.4–10 mm/day in rat [42,46], to 102 mm/day in chick [36]. Passive diffusion has been estimated to occur in the range of 5–6.7 mm/day [59,64,65]. A thorough review of active transport rates [1] reports that fast anterograde axonal transport occurs at a rate of 200–400 mm/day, while slow axonal transport occurs at either 0.2–0.01 mm/day (type A) or 2–8 mm/day (type B) [1,72–76]. The bulk anterograde rate found in the present study (80–90 mm/day) is at least 12 times faster than passive diffusion, at least 10 times faster than the upper bound of the slow active rate and 2–5 times slower than the fast active rate. Thus it is closer to the fast rate although it doesn't neatly fit within either group, similarly to the report in chick [36]. However, it is possible that the anterograde rate is faster than that we estimate here given the limitations of the methods we used. For example, we include the time for CTB to diffuse throughout the vitreous within the total duration to appear at the superior colliculus and we are limited further by the 'background' (noise and autofluorescence) intensity. The latter could possibly be improved by use of a more narrow-band emission filter (than that within the CSLO instrument). However, the CSLO method proved to be actually more sensitive than using microscopy with a narrower band emission filter, suggesting much of the fixed-tissue autofluorescence occurs within the same band as AlexaFluor-488 emission. It is also possible that signal amplification may result in faster anterograde transport rate estimates, such as might be accomplished by additional two- or three-step immunohistochemistry with a primary antibody against CTB. In summary, since these methods require a critical amount of CTB to reach the superior colliculus before it is detectable by either CLSO or microscopy, the anterograde estimate of 80 to 90 mm/day is likely conservative. Nevertheless, it should be possible to detect delayed or obstructed anterograde transport in experimental models of optic neuropathy using these methods; such studies are presently underway.

For retrograde axonal transport, this study found a rate of 136–191 mm/day, which is within the previously reported range of fast active retrograde axonal transport of 100–250 mm/day [1]. A previously estimated rate of 290 mm/day for retrograde transport of CTB has been reported in motor neurons of rats [46] and others report that the rate of retrograde transport of CTB was similar to their estimates of anterograde transport (102 mm/day) in chick [36]. Our estimates of retrograde rate fit between these previous studies. Rates of movement by membranous diffusion, such as occurs for the carbocyanine dyes, have been reported to require 3 days to reach the eye in the adult rat [64,65]. In contrast, our results indicate that CTB arrives at the eye ~3 hours after injection into the superior colliculus, which is about 24 times faster than membranous diffusion.

Fast anterograde transport is involved in the movement of synaptic vesicle proteins, kinesins and neurotransmitter metabolism enzymes, while fast retrograde axonal transport is involved with transport of endosomes, lysosomes, autophagosomes and neurotrophins, all critical for neuron survival [1,75,77–82]. Recently *in vitro* live-cell imaging [32] was used to show the dynamics of the axonal transport of BDNF in RGCs. The maximum retrograde rate of BDNF axonal transport was found to be 175 mm/day (i.e., 2.03 μm/s), which is equivalent to the retrograde rate of CTB transport observed *in vivo* in the present study.

The *in vivo* assay of retrograde transport developed in this study provides a potentially important advantage for use in longitudinal studies of axon transport alterations in experimental models of optic nerve degeneration. Recently it has been shown that during the early stages after RGC injury, including experimental glaucoma, RNFL retardance (measured by scanning laser polarimetry) declines prior to the onset of RNFL thinning (measured by optical coherence tomography) and that RGC-specific functional changes (measured by

#178418 - $15.00 USD Received 19 Nov 2012; revised 10 Jan 2013; accepted 28 Jan 2013; published 30 Jan 2013

electroretinography) accompany the early-stage retardance changes [83,84]. The selective reduction of RNFL retardance presumably reflects disruption of the axonal cytoskeleton (primarily microtubules, but perhaps also neurofilaments, microtubule associated proteins and actin) [85–87]. Disruption of the axonal cytoskeleton is likely to be associated with reduced axonal transport. The method developed in this study provides direct assessment of axonal transport in RGC axons, which is particularly important complementary information to imaging the structural integrity of the axonal cytoskeleton. The retrograde method also allows monitoring of RGC counts *in vivo* for about one month until CTB starts to fade, after which the retrograde transport assay can be applied again.

This study found that CTB is a good marker for axonal transport since it diffuses rapidly through the vitreous and superior colliculus and enables uptake and subsequent transport by cells over a large area (see Figs. 1, 2, 3). In comparison, the retrograde injections of Di-O and retrobeads did not diffuse well into the superior colliculus, fluorescence took much longer to arrive and accumulate in the eye and only a small number of RGCs fluoresced. However, one limitation of the general technique (with any tracer) is that the injections are not always successful with regards to complete coverage, so the injection site needs to be checked to confirm whether negative results are due to disrupted transport or a failed injection. The criteria for what constitutes a failed injection might be changed for different experiments depending on the precise outcome measure (i.e., coverage of CTB filling) required for the chosen analysis.

Intravitreal injection of CTB shows uptake into RGC somas, dendrites and axons (Fig. 1). The distribution of Gm1 receptors on RGCs is unknown for the adult vertebrate retina, so the putative site of CTB uptake is also unknown. However, the application of intravitreal colchicine prior to intravitreal CTB resulted in fluorescence of axons up to and including the neuroretinal rim of the optic disc, despite severely disturbed transport of CTB further up the anterior optic nerve, chiasm, tract and into the superior colliculus. This indicates it is likely that some amount of CTB uptake occurs along the intra-retinal axons since otherwise CTB should not have reached the optic disc. Alternatively, there may be some CTB diffusion within the axonplasm or incomplete transport blockade by colchicine in the intra-retinal axons compared to the axons within the distal optic nerve. Although some CTB uptake likely occurs along intra-retinal axons, the colchicine results show that the large majority of axon filling by CTB occurs via active, microtubule-dependent axonal transport.

In addition to being a marker of axonal transport, retrograde transport of CTB in the visual pathway results in the labeling of RGCs *in vivo*, which we demonstrate can also be visualized *in vivo*. Numerous other approaches have also been reported for visualization and monitoring of RGCs *in vivo*, all of which have powerful advantages over histological methods [88–105]. Both CSLO and microscopy methods were used to determine the success of the transport assays. The CSLO has the advantage of providing quantitative measurements *in vivo* for the retrograde assay, and of providing quick and simple post mortem measurements for both assays, compared to microscopy techniques involving extensive dissection or processing tissue for sections. The CSLO technique for imaging optic nerves, chiasm and superior colliculi is also better suited than microscopy for the post mortem anterograde assay as the field size, depth of field and working distance are all superior to the objective lenses available on most fluorescence microscopes. However, microscopy has the advantage of higher magnification and better visibility of RGCs in a flat-mounted retinal preparation, compared to CSLO where the entire retina is not perfectly in focus all at once. Nonetheless, the CSLO technique proved to be slightly more sensitive (less variable) than microscopy for the anterograde assay and showed high Spearman correlations. Similarly, there was a strong correlation between RGC counts obtained *in vivo* by CSLO and post-mortem by microscopy of retinal flat-mounts. These results indicate that the CSLO methods are valid for these axonal transport assays in future applications.

#178418 - $15.00 USD Received 19 Nov 2012; revised 10 Jan 2013; accepted 28 Jan 2013; published 30 Jan 2013

5. Conclusions

This study showed that anterograde and retrograde axonal transport of CTB is dependent on intact microtubules and occurs by fast active mechanisms. The findings show that these anterograde and retrograde assay methods are suitable for use in studying axonal transport in experimental rodent models of optic neuropathy including glaucoma. The anterograde assay *in vivo* is confounded because CTB uptake and transport along the intra-retinal axon cannot be differentiated using the current CSLO imaging technique. However, a promising alternative might be manganese-enhanced magnetic resonance imaging, to assay anterograde transport *in vivo* along the anterior visual pathway [106,107]. Alternatively, in the future, adaptive optics applied to CSLO might enable visualization of axonal transport directly (i.e., individual cargo molecules) and allow an instantaneous rate to be calculated [96,108]. Since we demonstrate here that retrograde transport is able to be assayed *in vivo*, it will be useful to develop this method for use in non-human primate models of experimental glaucoma to study axonal transport *in vivo* relative to other known clinical stages of the disease model.

Acknowledgments

The authors would like to thank Cory Szybala for guidance during the initial stereotactic surgeries and Chelsea Piper for assistance during some of the intravitreal injections. This study had funding support from the National Institutes of Health—National Eye Institute (R21EY021311) and the Legacy Good Samaritan Foundation, and equipment support from Heidelberg Engineering GmbH.